

Improved Privacy-Preserving PCA Using Space-optimized Homomorphic Matrix Multiplication

Xirong Ma*

*School of Software, Shandong University

May 30, 2023

Abstract

Principal Component Analysis (PCA) is a pivotal technique in the fields of machine learning and data analysis. It aims to reduce the dimensionality of a dataset while minimizing the loss of information. In recent years, there have been attempts to employ homomorphic encryption for privacy-preserving PCA algorithms, but their performance and accuracy are not satisfactory. This has prompted us to propose a more efficient solution. In this study, we present a novel approach for privacy-preserving PCA using an approximate numerical arithmetic homomorphic encryption scheme. We build our method upon a proposed PCA routine known as the PowerMethod, which takes the covariance matrix as input and produces an approximate eigenvector corresponding to the first principal component of the dataset. Our method surpasses previous approaches (e.g., Pandas CSCML 21) in terms of efficiency, accuracy, and scalability.

To achieve such efficiency and accuracy, we have implemented the following optimizations: (i) We optimized a homomorphic matrix multiplication technique (Jiang et al. SIGSAC 2018) that will play a crucial role in the computation of the covariance matrix. (ii) We devised an efficient homomorphic circuit for computing the covariance matrix homomorphically. (iii) We designed a novel and efficient homomorphic circuit for the PowerMethod that incorporates a systematic strategy for homomorphic vector normalization enhancing both its accuracy and practicality.

Our matrix multiplication optimization reduces the minimum rotation key space required for a 128×128 homomorphic matrix multiplication by up to 64%, enabling more extensive parallel computation of multiple matrix multiplication instances. Our homomorphic covariance matrix computation method manages to compute the covariance matrix of the MNIST dataset (60000×256) in 51 minutes. Our privacy-preserving PCA scheme based on our new homomorphic PowerMethod circuit successfully computes the top 8 principal components of datasets such as MNIST and Fashion-MNIST in approximately 1 hour, achieving an r^2 accuracy of 0.7 to 0.9, achieving an average speed improvement of over 4 times and offers higher accuracy compared to previous approaches.

1 Introduction

Principal Component Analysis (PCA) [Hot33], [Pea01] is a commonly used dimensionality reduction technique that maps high-dimensional data to a lower-dimensional space. PCA aims to reduce redundant information and noise in the dataset while extracting the most representative features. Specifically, PCA transforms the original data into a set of new orthogonal variables called principal components, which represent the directions of maximum variance in the original data. PCA finds widespread applications in data analysis and machine learning, including data preprocessing, feature extraction, data compression, and visualization. It helps us understand the relationships within a dataset and provides a simpler and more manageable representation. By reducing the dimensionality of the data, PCA enhances efficiency in analysis, while also reducing computational and storage costs, making it a highly useful tool in data analysis.

Cloud service providers offer various data analysis services to users, including outsourced computation scenarios such as cloud-based machine learning, which address limitations such as insufficient local computing resources and complex computational tasks. However, due to concerns about the trustworthiness of cloud storage, users are unable to perform analysis and processing of sensitive data

directly using cloud computing power. Instead, they need to add privacy protection measures to their data before outsourcing it to counter potential attacks from an untrusted cloud. Therefore, we believe that implementing a PCA algorithm with data confidentiality that can be executed in the cloud is meaningful and important for expanding privacy-preserving cloud services.

Homomorphic Encryption is an important privacy-preserving technique that allows computations to be performed on encrypted data without decryption. This technology helps protect data privacy while maintaining data usability, making it widely used in fields such as cloud computing and cross-domain computation. Numerous privacy-preserving machine learning algorithms based on homomorphic schemes have been designed, including privacy-preserving PCA schemes [LKS16], [RMY18], [Pan21] tailored for cloud service scenarios.

These existing homomorphic encryption-based privacy-preserving PCA methods utilized the iterative PowerMethod algorithm to compute the dominant eigenvector of the dataset's covariance matrix, which corresponds to the first principal component. This algorithm selects an initial approximation of the dominant eigenvector and continually applies the covariance matrix transformation to refine its approximation (see figure 1). We summarize two significant challenges that hindered the previous approaches in evaluating PowerMethod homomorphically:

1. Incapability to homomorphically compute the covariance matrix. PowerMethod necessitates the input of the dataset's covariance matrix, but previous schemes did not offer a homomorphic solution for computing the matrix. Instead, they resorted to alternative methods. Some required users to compute the covariance matrix locally which burdened the users with additional computational tasks and deviated from the original intent of cloud services. Others decomposed the covariance matrix transformation into dataset matrix transformations within PowerMethod to avoid explicit involvement of the covariance matrix but introduce increased computational complexity.
2. Significant accuracy loss caused by the lack of a systematic vector normalization strategy. In each iteration of PowerMethod, normalization is required to control the vector's length. In the homomorphic context, iterative algorithms are typically used to approximate the inverse square root function for normalization. The accuracy of these algorithms heavily relies on the selection of parameters such as the number of iterations and the evaluation range. Previous approaches failed to provide a universal and systematic rule for determining these parameter settings.

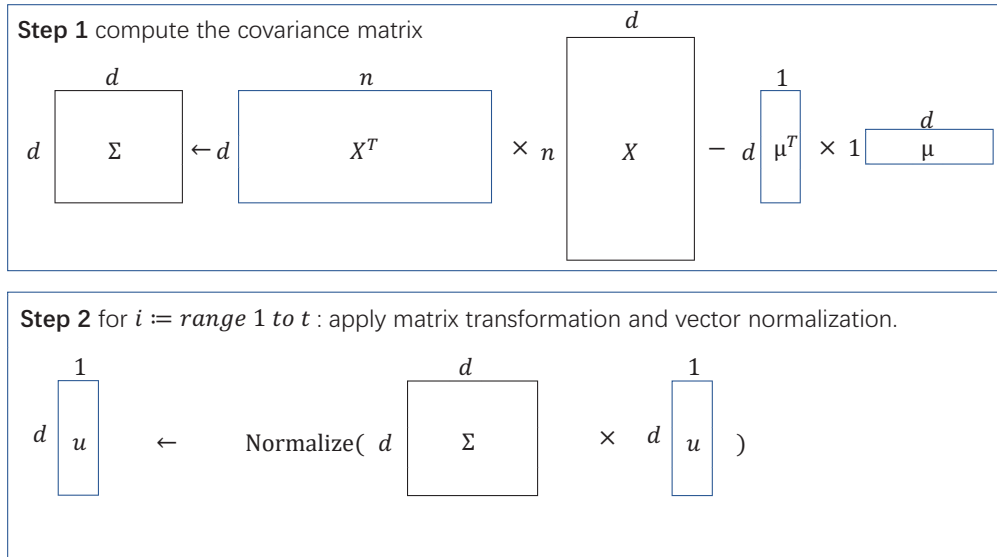


Figure 1: First principal component computation using PowerMethod

1.1 Our Results

We propose an efficient privacy-preserving PCA algorithm that overcomes the aforementioned obstacles. To achieve this, we make the following contributions.

Improved Matrix Multiplication (Section 4) In order to compute the covariance matrix, we first explored the use of a state-of-art homomorphic matrix multiplication algorithm combined with some existing optimization techniques. However, we encountered space limitations due to the large rotation key space required by the algorithm when attempting to perform parallel matrix multiplications for large datasets. This motivated us to seek ways to reduce the rotation key space for matrix multiplication while maintaining or even improving its computational efficiency.

Homomorphic Covariance Matrix Computation (Section 5) Leveraging the improved homomorphic matrix multiplication, we design a circuit for homomorphically computing the covariance matrix of large datasets. It takes advantage of parallel computation using multiple instances of matrix multiplication and exploits the symmetry of the covariance matrix to enhance efficiency.

Privacy-preserving PCA using Homomorphic PowerMethod (Section 6) PowerMethod consists of two main components: covariance matrix transformation and vector normalization. We first design efficient computational circuits for covariance matrix transformation. Next, for vector normalization, we employ an iterative algorithm approximating the square root inverse function. We discuss in detail the selection of evaluation range and number of iterations for the iterative algorithm, enabling homomorphic PowerMethod to produce more accurate results. Finally, we present the process of performing privacy-preserving PCA utilizing our homomorphic PowerMethod circuit.

Implementation (Section 7) We compare our proposed solution with existing approaches in terms of performance, highlighting that our algorithm outperforms previous methods in terms of computational efficiency, precision, and scalability.

2 Related Work

2.1 Homomorphic Encryption Matrix Multiplication

Currently, homomorphic encryption matrix multiplication algorithms can be roughly divided into two categories. The first category encodes the matrices into the native plaintext space of the homomorphic encryption scheme [DMY16, MRDY21]. These approaches require small computational complexity but lack composability, meaning that the output of the algorithm has a different form from the input, making it difficult to apply subsequent computations.

The second category is based on homomorphic encryption linear transformations [HS14, HS18, RMY18, JKLS18, WH19]. These approaches utilize the rotational properties of ciphertext slots to permute the matrix elements within the ciphertext, thereby achieving matrix multiplication. Among them [JKLS18] initially proposed a matrix multiplication scheme based on approximate numerical arithmetic homomorphic encryption schemes [CK18]. Its time complexity is dominated by approximately $O(n)$ ciphertext multiplications and $O(\sqrt{n} + n)$ ciphertext rotations (where n is related to the matrix size), making it one of the matrix multiplication schemes with optimal asymptotic complexity for square matrices in this category. [JLK⁺22] migrates it to an approximate numerical arithmetic homomorphic encryption variant that supports the hypercube structure in the plaintext space, simplifying some of its steps and further improving the runtime speed.

However, few have systematically discussed the space complexity of homomorphic matrix multiplication which is an important performance metric in parallel computation scenarios. We believe it is necessary to explore this issue because the parallel computation of multiple homomorphic matrix multiplication instances is crucial for accelerating large-scale matrix operations involving multiple ciphertexts. Our subsequent optimizations will be based on the matrix multiplication scheme proposed in [JKLS18], focusing on optimizing the speed and space utilization of parallel computation with multiple homomorphic matrix multiplication instances.

2.2 Privacy-preserving PCA in cloud computing scenario

The initial attempts at performing PCA on the BGV-like homomorphic encryption scheme [BGV14] were made by [LKS16] and [RMY18]. They proposed using an iterative algorithm called PowerMethod to compute principal components in a homomorphic encryption setting. The PowerMethod iteratively

computes $\mathbf{v} \leftarrow \text{Cov} \cdot \mathbf{v}$, and it can be proven that \mathbf{v} converges to the dominant eigenvector of the covariance matrix Cov after a finite number of steps, where the dominant eigenvector is equivalent to a principal component. However, they found the homomorphic computation of the covariance matrix to be inefficient for arbitrary sample sizes. Therefore, they required the client (of cloud service) to compute and send the encryption of $\sum \mathbf{x}_i^T \mathbf{x}_i$ (where \mathbf{x}_i represents the row vector form of the samples in the dataset X), which not only cause the computation burden on the user but also becomes trivial because PowerMethod is no harder than computing $\sum \mathbf{x}_i^T \mathbf{x}_i$ in plaintext space. Furthermore, due to the limitations of the BGV scheme, which only supports homomorphic operations on modular integers, all PCA schemes based on this homomorphic encryption cannot normalize the approximate eigenvector \mathbf{v} during iterations and are prone to overflow.

Subsequently, Panda migrated the Power Method to an approximate numerical homomorphic encryption scheme [Pan21]. The PowerMethod in this scheme is done by iteratively computing $\mathbf{v} \leftarrow 1/N \cdot X^T(X\mathbf{v})$ (where X is the centered dataset), rather than directly computing the covariance matrix transformation. This made the complexity of the PowerMethod dependent on the sample size of the dataset rather than the size of the covariance matrix, which is inefficient for datasets with a large number of samples.

Furthermore, Since the approximate numerical homomorphic encryption supports approximate computation on complex numbers, [Pan21] is able to apply approximation of inverse square-root function to normalize the approximate eigenvector \mathbf{v} . However, [Pan21] provides only one possible implementation of the iterative algorithm for the inverse square-root function without demonstrating how to choose the evaluation interval and the number of iterations when faced with various datasets. Reasonable selection of these critical details will directly affect the correctness and practicality of the scheme.

In addition, The aforementioned approaches lack discussions on scalability. The datasets used in their experiments could be loaded with just a few homomorphic encryption ciphertexts. However, in real-world scenarios, datasets often have hundreds of features and thousands of data points, requiring hundreds of ciphertexts to be loaded. This motivates us to explore homomorphic PCA schemes suitable for larger-scale datasets.

3 Preliminaries

3.1 General Notation

We will use italic letters, such as a , to represent polynomial elements or numbers. We use bold letters, such as \mathbf{a} , to represent vectors, and uppercase letters, such as A , to represent matrices. The symbols \oplus and \odot denote element-wise addition and multiplication, respectively, also known as Hadamard addition and multiplication. The notation $\rho(\mathbf{a}; k)$ represents the result of cyclically left-shifting (or rotating) the components of vector \mathbf{a} by k positions. We use $\Phi_M(X)$ to denote the M -th cyclotomic polynomial and denote its $N = \varphi(M)$ roots as $\zeta_1, \zeta_3, \dots, \zeta_{\varphi(M)}$, where $\zeta_i = \zeta_1^i$. The symbol R represents the cyclotomic polynomial ring $\mathbb{Z}[X]/\Phi_M(X)$, and $R * Q_L$, where $Q_L = q_0 \times q_1 \times \dots \times q_L$ is the product of several prime numbers q_i . In this way, the elements of the ring $R * Q_L$ can be uniquely represented in the RNS field as $R_{q_0} \times R_{q_1} \times \dots \times R_{q_L} \cong R_{Q_L}$. Additionally, we use $(\mathbb{Z}/q\mathbb{Z}, +)$ to represent a modulo q additive group, where we may abuse the notation $(-q/2, q/2)$ and $[0, q-1]$ to refer to two different representations of the residue class. We define $[a]_q$ as the result of reducing a modulo q that falls into $(-q/2, q/2)$, and $a \bmod q$ as the result falling into $[0, q-1]$.

3.2 Homomorphic Encryption for Arithmetic of Approximate Numbers

Homomorphic encryption is a cutting-edge field in cryptography and serves as a powerful component for privacy-preserving computations. Cheon et al. proposed the Homomorphic Encryption for Arithmetic of Approximate Numbers [CK18] known as the CKKS scheme, which is a leveled homomorphic encryption scheme relying its security on the hardness of Ring Learning With Error(RLWE) problem. One of the distinguishing features of CKKS is its ability to perform computations on encrypted data in a continuous domain, allowing for efficient operations on real or complex numbers. This is achieved by leveraging a technique called approximate computing, which trades off precision for efficiency.

We will build our privacy-preserving PCA scheme upon a full-Residue Number System (RNS) variant of the CKKS scheme [CHK⁺19] implemented in the Lattigo library [lat22]. This variant allows efficient polynomial multiplication by representing polynomials in both the RNS and NTT (Number Theoretic Transform) domains. We will now briefly introduce the full-RNS CKKS scheme, consisting of four routines: the general routine, addition routine, multiplication routine, and rotation routine. More detailed information about full-RNS CKKS is placed in Appendix.

General routine

This part introduces the parameter and keys generation for full-RNS CKKS, the encoding method to convert a complex vector to a native plaintext form, and the encryption method to convert plaintext to ciphertext.

Parameter Generation Setparams(N, b, σ) sets $M = 2N$ and selects the M -th cyclotomic polynomial $\Phi_M(X) = X^N + 1$. Two sets of prime numbers $q_i | i = 0, \dots, L$ and $p_i | i = 0, \dots, \alpha - 1$ are chosen such that their products are at most b bits. These primes satisfy $q_i, p_i \equiv 1 \pmod{2N}$. Let $Q_L = \prod_{i=0}^L q_i$ and $P = \prod_{i=0}^{\alpha} p_i$. The ring $R_{Q_L} = \mathbb{Z}[X]_{Q_L} / \Phi_M(X)$ is referred to as the plaintext space of the CKKS scheme. The distribution over R for generating the secret key is denoted as $R \leftarrow \chi_s$, and the error distribution over R as $R \leftarrow \chi_e$, which is a truncated discrete Gaussian distribution with standard deviation σ .

Encoding: Encode($\mathbf{z}, \Delta, n, \ell$) takes a message vector $\mathbf{z} \in \mathbb{C}^n$, where $1 \leq n < N$ and n divides N , and converts it to a plaintext polynomial $m \in R_{Q_\ell}$. To prevent a significant precision loss in the conversion, a scaling factor Δ is applied on the message.

Decoding: Decode(m, Δ, n, ℓ) takes a plaintext polynomial $m \in R_{Q_\ell}$ as input and converts it to a message vector $\mathbf{z} \in \mathbb{C}^n$, where $1 \leq n < N$ and n divides N . The decoding process is the inverse operation of encoding.

Secret Key Generation: SecKeyGen(\cdot) samples $s \leftarrow \chi_s$ and outputs the secret key s .

Public Key Generation: PubKeyGen(s) samples $e \leftarrow \chi_e$ and $a \in_u R_{Q_L}$, and outputs $(-as + e, a)$.

Encryption: Enc(m, pk) takes a plaintext polynomial $m \in R_{Q_\ell}$ and a public key $pk \in R_{Q_L}^2$ as input. It samples $a \in R_{Q_\ell}$ and computes and outputs $(a \cdot pk_0, a \cdot pk_1) + (m + e_0, e_1) \in R_{Q_\ell}^2$.

Decryption: Dec(c, sk) takes a ciphertext $c \in R_q^2$ and a secret key sk as input and outputs a plaintext polynomial $m' \in R$. It computes and outputs $m' = c_0 + c_1 \cdot sk \in R_{Q_\ell}$.

Besides the public key and secret key for encryption and decryption, switching keys are required for some homomorphic evaluation routines. They are used to convert a ciphertext under secret s to the ciphertext under another secret s' without changing its underlying plaintext.

Switch Key Generation: SwitchKeyGen(s, s', \mathbf{b}) for $\mathbf{b} \in \mathbb{Z}^\beta$ a vector representation of a certain integer decomposition basis, SwitchKeyGen takes in s, s' and outputs a vector with β elements in $R_{PQ_L}^2$ as the switching key swk .

Key Switching: KeySwitch(c, swk) takes a polynomial $a \in R_{Q_\ell}$ and a switching key swk as input. It first decomposes a with respect to the decomposition basis \mathbf{b} of swk , i.e., $a = \langle \mathbf{a}, \mathbf{b} \rangle$. Then, it computes and returns $(a_0, a_1) = \lfloor P^{-1} \cdot \langle \mathbf{a}, swk \rangle \rfloor \pmod{Q_\ell}$.

Addition routine

This part introduces the function provided by full-RNS CKKS to achieve homomorphic addition among plaintexts and ciphertexts.

Plaintext Addition: PAdd(c, m) takes a plaintext polynomial $m \in R_{Q_\ell}$ and a ciphertext $c \in R_{Q_\ell}^2$ as input, both having the same scaling factor. It outputs a ciphertext $c' = c + (m, 0)$.

Ciphertext Addition: Add(c_1, c_2) takes two ciphertexts $c_1, c_2 \in R_{Q_\ell}^2$ with the same scaling factor as input and outputs $c_1 + c_2$.

Multiplication routine

This part introduces the function provided by full-RNS CKKS to achieve homomorphic multiplication among plaintexts and ciphertexts.

Plaintext Multiplication: PMult(c, m): Given a plaintext polynomial $m \in R_{Q_\ell}$ and a ciphertext $c \in R_{Q_\ell}^2$ with scaling factors Δ and Δ' respectively, compute and return $c' = (c_0 \cdot m, c_1 \cdot m)$. The resulting ciphertext c' has a scaling factor of $\Delta\Delta'$.

Ciphertext Multiplication: Mult(c_1, c_2): For ciphertexts c and c' with scaling factors Δ and Δ' respectively, compute $(d_0, d_1, d_2) = (c_0 c'_0, c_0 c'_1 + c_1 c'_0, c_1 c'_1)$ and return $d = (d_0, d_1) + \text{SwitchKey}(d_2, \text{rlk}) \in$

$R_{Q_\ell}^2$ as the resulting ciphertext. The resulting ciphertext d has a scaling factor of $\Delta\Delta'$.

Level Dropping: $\text{Drop}(c, k)$: Given a ciphertext $c \in R_{Q_\ell}^2$, return $c \in R_{Q_{\ell-k}}^2$.

Rescaling: $\text{Rescale}(c)$: For a ciphertext $c \in R_{Q_\ell}^2$ with scaling factor Δ , return $\lfloor q_\ell^{-1} \cdot c \rfloor$. The resulting ciphertext has a scaling factor of Δ/q_ℓ .

The rescale operation is commonly used to limit the error in the ciphertext by transferring the encrypted data from a ring with a large modulus to a ring with a smaller modulus, reducing the error introduced by multiplications.

Rotation routine

This part introduces the function provided by full-RNS CKKS to achieve homomorphic position shifting in a ciphertext. Specifically, full-RNS CKKS allows us to homomorphically rotate the position of the components of the underlying plain complex vector in a ciphertext.

Rotation: $\text{Rot}(c_1, k)$: Given a ciphertext $c \in R_{Q_\ell}^2$ and a rotation key rtk_k , compute and output $(c_0^{5^k}, 0) + \text{SwitchKey}(c_1^{5^k}, \text{rtk}_k)$. This ciphertext represents the result of rotating all components of the message vector $\mathbf{z} \in \mathbb{C}^{N/2}$ encrypted by c to the left by i steps (or positions), denoted as $\mathbf{z}' = \rho(\mathbf{z}; i)$.

3.3 Homomorphic Matrix Operation

We will primarily discuss the matrix multiplication scheme and its optimization proposed in [JKLS18] for approximate numerical homomorphic encryption. Since this scheme is based on homomorphic linear transformation, we will first introduce the concept of homomorphic linear transformation and then discuss matrix multiplication.

3.3.1 Homomorphic Linear Transformation

Halevi et al. first proposed an approach to achieve linear transformations in the context of homomorphic encryption [HS14]. They pointed out that any matrix transformation $U\mathbf{m}$ can be represented as:

$$U \cdot \mathbf{m} = \sum_{0 \leq \ell < n} (\mathbf{u}_\ell \odot \rho(\mathbf{m}; \ell)) \quad (1)$$

where \mathbf{u}_ℓ represents the ℓ -th diagonal vector of U : $\mathbf{u}_\ell = (U_{0,\ell}, U_{1,\ell+1}, \dots, U_{n-1,(\ell+n-1) \bmod n})$. By associating \mathbf{m} with the ciphertext vector and U with the plaintext matrix in (1), we can achieve a linear transformation between the ciphertext vector and the plaintext matrix using this approach. [HS18] proposed an optimization algorithm called Baby Step Giant Step (BSGS) for this linear transformation method: For a linear transformation $U \cdot \mathbf{m}$ of an n^2 -dimensional vector, if the indices of all non-zero diagonal vectors of U are bounded by d , where $0 \leq d < n^2$, and $d = d_1 d_2$, then for any non-zero diagonal vector index $-d \leq k < d$, we have $k = d_1 i + j$, where $-d_2 < i < d_2$, $0 < j < d_1$. Consequently, (1) can be rewritten as an operation with two nested loops: the outer loop running d_2 times and the inner loop running d_1 times.

$$\begin{aligned} U\mathbf{m} &= \sum_{-d_2 < i < d_2, 0 \leq j < d_1} (\mathbf{u}_{d_1 \cdot i + j} \odot \rho(\mathbf{m}; d_1 \cdot i + j)) \\ &= \sum_{-d_2 < i < d_2} \rho \left(\sum_{0 \leq j < d_1} (\rho(\mathbf{u}_{d_1 \cdot i + j}; -d_1 \cdot i) \odot \rho(\mathbf{m}; j)); d_1 \cdot i \right) \end{aligned} \quad (2)$$

Under this optimization, one instance of ciphertext linear transformation requires $O(d_1 + d_2)$ rotations. BSGS performs even better when the indices of diagonal vectors form an arithmetic progression. Specifically, for any non-zero diagonal vector index k , there exists a positive integer a such that $k = a \cdot q$, where q is an integer with absolute value less than $d = d_1 d_2$. Thus, we have $k = a(d_1 \cdot i + j)$, where

$-d_2 < i < d_2$ and $0 < j < d_1$. In this case, (2) can be rewritten as:

$$\begin{aligned} U\mathbf{m} &= \sum_{-d_2 < i < d_2, 0 \leq j < d_1} (\mathbf{u}_{a \cdot (d_1 \cdot i + j)} \odot \rho(\mathbf{m}; a \cdot (d_1 \cdot i + j))) \\ &= \sum_{-d_2 < i < d_2} \rho \left(\sum_{0 \leq j < d_1} (\rho(\mathbf{u}_{a \cdot (d_1 \cdot i + j)}; -a \cdot d_1 \cdot i) \odot \rho(\mathbf{m}; a \cdot j)); a \cdot d_1 \cdot i \right) \end{aligned} \quad (3)$$

Further optimization can be achieved by analyzing the rotation operations. Halevi et al. introduced a ciphertext rotation optimization technique called "hoisting" in [HS18]. They pointed out that if multiple rotations with different step sizes are performed on the same ciphertext, and the rotation keys corresponding to each step are provided, then these rotation operations can share some internal sub-operations, thereby reducing the total number of operations. Specifically, hoisting allows the four internal operations that constitute a rotation to be performed in the following order: **Decompose**(ct) - \hookrightarrow **MultSum**(ct, rtk) - \hookrightarrow **Permute**(ct) - \hookrightarrow **ModDown**(ct). Here, **Decompose** and **ModDown** involve number-theoretic transforms and Chinese remainder theorem basis extensions, which dominate the computational complexity of rotation operations. The rotation keys are only involved in the **MultSum**. Therefore, if multiple rotations with different step sizes are required on the same ciphertext, and all the corresponding rotation keys are available, these rotations can share the result of **Decompose**(ct).

Bossuat et al. applied the hoisting idea to the BSGS-optimized linear transformation algorithm mentioned above in [BMTPH21]. They proposed applying hoisting to the rotations $\rho(\mathbf{m}; a \cdot j), 0 \leq j \leq d_1$ in (3). Specifically, instead of executing the complete hoisting rotation operation, they deferred the final step, **ModDown**, multiplied the intermediate rotation results, which were still in R_{PQ_ℓ} , with the corresponding pre-rotated diagonal vectors $\rho(\mathbf{u}_{a \cdot (d_1 \cdot i + j)}; -a \cdot d_1 \cdot i)$ and then aggregated all the products before finally applying **ModDown** operation to the aggregated result. This optimization method is referred to as the double-hoisting technique. It reduces the computational complexity of the BSGS-optimized linear transformation from $(n_2 + n_1) \cdot (\mathbf{MultSum} + \mathbf{ModDown} + \mathbf{Decompose} + \mathbf{Permute})$ to $(n_2 + n_1) \cdot (\mathbf{MultSum} + \mathbf{Permute}) + (n_2 + 1) \cdot (\mathbf{Decompose} + \mathbf{ModDown})$.

For the double hoisting technique, the choice of inner loop count d_1 can be adjusted to balance space complexity and running speed. The space complexity comprises two primary components: the d_1 pre-rotated ciphertexts for BSGS inner loop and the rotation keys that can be shared among instances of the same linear transformation. It is evident that a smaller inner loop results in fewer pre-rotated ciphertexts but a slower speed. Conversely, a larger inner loop leads to more extensive use of pre-rotated ciphertexts but faster speed. However, the number of rotation keys is minimized when the inner and outer loops are closest to each other.

In the subsequent discussion, we assume that all the rotation keys required for performing any homomorphic encryption linear transformation are stored in memory prior to the computation. This is also the current implementation strategy in Lattigo. Although it is theoretically possible to load a key into memory only when it is needed for computation and release it afterward to control a smaller memory footprint for keys, we do not recommend this practice. It would incur additional time for disk read/write operations and disrupt the compactness of the storage structure. Especially, it would significantly slow down the speed of consecutive linear transformation calculations. Moreover, when considering parallel computation of multiple linear transformations, controlling the execution order of threads and the access order to temporary retrieved keys would become increasingly difficult and complex, and the space benefits obtained would not compensate for the loss in computational speed.

3.3.2 Homomorphic Matrix Multiplication by Jiang et al.

Jiang et al. proposed a homomorphic matrix multiplication approach based on the aforementioned linear transformation algorithm and its BSGS optimization [JKLS18]. Due to the SIMD property of CKKS-like schemes, a square matrix A of size $n \times n$ can be encoded as a vector \mathbf{a} with n^2 components using the row ordering encoding, as long as there are enough ciphertext slots for the message. For simplicity, let n^2 be equal to the number of available slots in a ciphertext (recall that $N/2$ is the maximum number of available slots, where N is the degree of the cyclotomic polynomial $\Phi_M(X)$). Considering the multiplication of matrices A and B , Jiang et al. first apply a series of different linear transformations to the corresponding encoding vectors \mathbf{a} and \mathbf{b} , and then use coordinate-wise multiplication to pairwise multiply the transformed results and aggregate them to obtain the encoding vector \mathbf{c} of the matrix AB as follows:

$$\mathbf{c} = \sum_{k=0}^{n-1} (C^k Z \mathbf{a}) \odot (R^k T \mathbf{b}) \quad (4)$$

Here, C , Z , R , and T are different permutation matrices. They also designed permutation matrix transformations for matrix transposition: $\mathbf{a}' = G\mathbf{a}$, where G is a specific permutation matrix and \mathbf{a}' represents the transpose A^T of the matrix A represented by \mathbf{a} . The BSGS algorithm is employed for the transformations Z, T, G to greatly enhance efficiency. However, they treated BSGS as a black-box operation without considering the aforementioned hoisting techniques for internal optimization. As a result, the trade-off between space and speed was not discussed in their research.

3.4 Principal Component Analysis using PowerMethod

Principal Component Analysis (PCA) is frequently employed for the dimensionality reduction of a dataset. Its fundamental concept involves identifying orthogonal axes that maximize the variance of the dataset projected onto these axes, which are referred to as principal components. Finding the top k principal components is equivalent to determining the k largest eigenvectors and eigenvalues of the covariance matrix of the dataset.

Recall figure 1, the covariance matrix Σ of the dataset is given by $\Sigma = \frac{1}{N}X^T X - \mu\mu^T$, where $u^T = \frac{1}{N} \sum_{i=0}^{N-1} \mathbf{x}_i^T$. The Power Method is an approximate algorithm for computing the largest eigenvector, as outlined in Algorithm 1. Since the Power Method can only calculate the dominant eigenvector, the EigenShift technique is used to shift the covariance matrix in terms of eigenvectors. It takes the covariance matrix and the top k eigenvectors as inputs and outputs a new covariance matrix, where the $(k+1)$ -th dominant eigenvector becomes the largest eigenvector. By combining these two algorithms, we can compute the top principal components of the dataset.

Algorithm 1 PowerMethod

Input: Σ : covariance matrix of dataset X ; T : number of iterations;

Output: \mathbf{u}_1, λ_1 : dominant eigen-vector of Σ and its eigen-value

- 1: Choose a random vector $\mathbf{v}^{(0)}$ of size d
 - 2: **for** $i = 1$ to T **do**
 - 3: $\mathbf{v}^{(i)} \leftarrow \Sigma \mathbf{v}^{(i-1)}$
 - 4: $\mathbf{v}^{(i)} \leftarrow \mathbf{v}^{(i)} / \|\mathbf{v}^{(i)}\|$
 - 5: **end for**
 - 6: **return** $\mathbf{u}_1 = \mathbf{v}^{(T)}$ and $\lambda_1 = \|\mathbf{v}^{(T)}\| / \|\mathbf{v}^{(T-1)}\|$
-

Algorithm 2 EigenShift

Input: Σ : covariance matrix of X ; $\{\mathbf{u}_i, \lambda_i\}$: i -th dominant eigenvector of Σ and its eigenvalue

Output: Σ_k : k -shifted covariance matrix of X

- 1: **for** $i = 1$ to $k-1$ **do**
 - 2: $\Sigma_{i+1} = \Sigma_i - \lambda_i \mathbf{u}_i \mathbf{u}_i^T$
 - 3: **end for**
 - 4: **return** Σ_k
-

3.5 Iterative algorithm of inverse square root function

The Power Method algorithm for computing principal components, as mentioned above, requires the normalization of the approximate eigenvectors $\mathbf{v}^{(i)}$ during its process. This involves implementing the Inverse SquareRoot function. Since existing fully homomorphic schemes only support addition, multiplication, and rotation operations, we cannot directly evaluate the square root and inverse functions on ciphertexts. One feasible approach is to use iterative algorithms to approximate the Inverse SquareRoot function, where methods such as GoldSchmidt's Algorithm and Newton's Method (Algorithm 3 and 4) can be employed. These methods take the desired point for evaluation and an appropriate

initial estimation of the inverse square root as input and output a more accurate result after a finite number of iterations. Providing a good initial approximation can result in better convergence speed. In [Pan22], an approach of piecewise linear function approximation is used to compute the initial approximation for Newton’s Method, which iteratively approximates the exact inverse square root value. In [QX], the use of Taylor expansions or rational polynomial approximations is suggested to obtain a better initial value, reducing the number of iterations needed in Newton’s Method to approximate the exact value. For any given number of iterations, it can be proven that the results of algorithm 3 and 4 are equivalent(theorem 1). However, GoldSchmidt’s Algorithm requires updating two values in each iteration, resulting in a higher number of modulus switching operations compared to Newton’s Method. In subsequent discussions, we will use the term ”Inverse SquareRoot(InvSRT) iteration algorithm” to refer to these two specific methods, as they do not have any other differences in this context.

Algorithm 3 Goldschmidt’s Algorithm

Input: x_0 : input of inverse square root. y_0 : The initial approximation at point x_0

Output: A more precise approximation at point x_0

```

1:  $g_0 \leftarrow x_0 \cdot y_0$ 
2:  $h_0 \leftarrow y_0/2$ 
3: for  $i = 1$  to  $d$  do
4:    $r_i \leftarrow 0.5 - g_{i-1}h_{i-1}$ 
5:    $g_i \leftarrow g_{i-1} + g_{i-1}r_{i-1}$ 
6:    $r_i \leftarrow h_{i-1} + h_{i-1}r_{i-1}$ 
7: end for
8: return  $2h$ 

```

Algorithm 4 Newton’s Method

Input: x_0 : input of inverse square root. y_0 : The initial approximation at point x_0

Output: y_d : A more precise approximation at point x_0

```

1: for  $i = 1$  to  $d$  do
2:    $y_i \leftarrow \frac{1}{2}y_{i-1}(3 - x_0y_{i-1}^2)$ 
3: end for
4: return  $y_d$ 

```

Theorem 1. *For any number of iterations k , algorithm 3 and 4 yield the same result.*

Proof. Assuming that for any iteration round less than k , we have $h_i = 1/2y_i$ and $g_i = x_0y_i$ for the algorithms mentioned above. For iteration round $i = 1$, the above result holds. For iteration round $i = k$, we have $h_k = h_{k-1} + h_{k-1}(0.5 - g_{k-1}h_{k-1}) = 1/2y_{k-1} + 1/2y_{k-1}(0.5 - x_0y_{k-1} \cdot 1/2y_{k-1}) = 1/2y_k$, and $g_k = g_{k-1} + g_{k-1}(0.5 - g_{k-1}h_{k-1}) = x_0y_{k-1} + x_0y_{k-1}(0.5 - 1/2x_0y_{k-1}^2) = x_0y_k$. \square

4 Improved Homomorphic Matrix Multiplication

Since we will use homomorphic matrix multiplication presented by Jiang et al. to compute the covariance matrix, we need to equip it with hoisting optimizations to improve its speed. Moreover, we need to check its performance in the parallel computation scenario. Thereby, in this section, we will first analyze the rotation complexity of the matrix multiplication optimized by hoisting techniques, and discuss its space complexity in the parallel computation scenario (section 4.1). We will see that the matrix multiplication with hoisting requires a large rotation key space that may occupy the memory and affect the performance of parallel computation. Thus two kinds of key space reduction methods will be introduced in subsections 4.2 and 4.3.

4.1 Hoisting Optimization in Matrix Multiplication

4.1.1 Rotation complexity and rotation key space analysis

The hoisting technique will be applied to the following linear transformations involved in the $n \times n$ matrix multiplication: $Z, T, \{C^k, R^k | 1 \leq k < n\}$. Our initial focus will be on Z and T . The matrix

Z comprises $2n - 1$ non-zero diagonal vectors with indices ranging from $-n + 1$ to $n - 1$. On the other hand, matrix T consists of only n non-zero diagonal vectors, with indices $k \cdot n$ where $0 \leq k < n$. Both Z and T exhibit a well-behaved arithmetic progression in the indices of the non-zero diagonal vectors. This property enables the BSGS algorithm to reduce the number of the rotations from $O(n)$ to $O(n_1 + n_2)$, where n_1, n_2 denotes the inner and outer loop count.

Scheme	LinTrans	MinRotKeys	Complexity(Rotations)
Origin	Z	$2n_2$	$(n_1 + 2n_2) \cdot (MS + Pm + Dp + MD)$
Optimized	Z	$n_1 + 2n_2 - 2$	$(n_1 + 2n_2) \cdot (MS + Pm) + (2n_2 + 1) \cdot (Dp + MD)$
Origin	T	n_2	$(n_1 + n_2) \cdot (MS + Pm + Dp + MD)$
Optimized	T	$n_1 + n_2 - 2$	$(n_1 + n_2) \cdot (MS + Pm) + (n_2 + 1) \cdot (Dp + MD)$
Origin	$\{C^k 0 \leq k < n\}$	1	$(2n - 2)(Dp + MS + Pm + MD)$
Optimized	$\{C^k 0 \leq k < n\}$	$n_{Z1} + 1$	$2Dp + (2n - 1)(MS + Pm) + (n)MD + (Dp + MD)2n/n_{Z1}$
Origin	$\{R^k 0 \leq k < n\}$	0	$(n - 1)(Dp + MS + Pm + MD)$
Optimized	$\{C^k 0 \leq k < n\}$	n_{T1}	$(n - 1)(MS + Pm + MD) + (n/n_{T1} + 1)Dp$

Table 1: Rotation Complexity and Minimal Rotation Keys requirement Comparison between BSGS and dh-BSGS scheme for Z , T linTrans. n_{Z1}, n_{T1} denote the inner loop count of Z and T transformation.

For $1 \leq k < n$, the transformation C^k has only two non-zero diagonal vectors: k and $k - n$, while R^k has only one non-zero diagonal vector: $n \cdot k$. Due to the scarcity of non-zero diagonals in these transformations, the optimization effect of BSGS on these transformations is minimal, and utilizing equation 1 is sufficient for their computation. However, we can still enhance their efficiency using the hoisting technique. We observe that in double-hoisting, all the rotation step sizes used for the inner loop of T precisely form a subsequence of the non-zero diagonal indices in the set $R^k | 0 \leq k < n$. Similarly, for the inner loop of Z , all the rotation step sizes form a subsequence of the non-zero diagonal indices in the set $C^k | 0 \leq k < n$. This implies that the rotations keys of Z and T can be reused for the transformations $C^k, R^k | 0 \leq k < n$ to achieve optimization through hoisting.

In particular, for the transformations C^k with two non-zero diagonal vectors, we can emulate the strategy used in double-hoisting by deferring the final **ModDown** operation in the rotations. Instead, we perform the multiplication of hoisted ciphertext with the corresponding plaintext diagonal vectors, aggregate the results, and then apply **ModDown** to the aggregated value. A detailed comparison of rotation complexity between matrix multiplication with hoisting and the original scheme in [JKLS18] is presented in Table 4.1.1.

4.1.2 Parallelizability of matrix multiplication and runtime space complexity analysis

Let us begin with the analysis of the rotation key space required by a matrix multiplication with hoisting techniques. Following section 4.1.1, we can observe that the minimal number of rotation keys required depends on the number of keys required by Z and T transformation. If we denote n_{Z1}, n_{Z2} (and n_{T1}, n_{T2}) as the inner loop count and outer loop count of Z (and T), then the total number of rotation keys required in matrix multiplication is $n_{Z1} + 2n_{Z2} + n_{T1} + n_{T2} + 3$. When considering a concrete scheme with parameters set as $n = 128, n_{Z1} = n_{T1} = 16, \log(N) = 15, \log(Q_{LP}) = 520$, the total rotation keys take up a large space of x MB. Such a large space may occupy the memory and hurt the performance of parallel computation since each instance of linear transformation imposes a runtime space requirement for caching intermediate-hoisted ciphertexts. Readers can be more aware of this problem in the following discussion of different parallel computation scenarios of matrix multiplication.

1. Internal parallelizability: The transformation $C^k Z \mathbf{a}$ and $R^k T \mathbf{b}$ in equation (4) can be computed in parallel. This imposes a maximum space requirement for caching $n_{Z1} + n_{T1}$ intermediate-hoisted ciphertexts. With the concrete settings aforementioned, a single internally parallel matrix multiplication instance can have a maximum of 32 intermediate ciphertexts, occupying a total of 180 MB.
2. Multi-instance parallel computation: Considering the parallel computation of multiple matrix multiplication instances, the total intermediate ciphertexts could require a significant amount of

memory. For instance, performing parallel computation on 10 matrix multiplication instances would require nearly 2 GB of space.

3. "One-to-many" parallel computation: In this scenario, matrix A is multiplied with multiple different matrices $\{B_i | i = 1, 2, \dots, d\}$. We can consider the following two pre-computation strategies to reduce the time for this scenario:
 - (a) Precompute and store $Z\mathbf{a}$ (or $T\mathbf{a}$), and compute the remaining steps of equation (3) in parallel with each B_i . The space requirement for this approach is $n_{Z1} + d \cdot n_{T1}$ (or $n_{T1} + d \cdot n_{Z1}$) ciphertexts.
 - (b) Precompute and store $\{C^k Z\mathbf{a} | k = 0, \dots, n\}$ (or $\{R^k T\mathbf{a} | k = 0, \dots, n\}$), and then compute the remaining steps of equation (3) in parallel for each B_i . The space requirement for this approach is $n + d \cdot n_{T1}$ (or $n + d \cdot n_{Z1}$) ciphertexts. The latter approach saves more time but has a higher space requirement.

4.1.3 Summary

We equipped matrix multiplication with hoisting techniques and discussed its computation and space complexity, where we observed that a large number of rotation keys can consume memory and impact parallel computational efficiency when the space resource is limited. To address this problem, we propose two techniques. The first technique is a simple key substitution method that effectively reduces the number of keys used in the Z, T 's inner loop but compromises the integrity of hoisting, resulting in increased speed loss as the number of keys decreases. This technique has only a marginal effect when the number of inner loop iterations is small.

The second technique involves diagonal vector convergence decomposition of Z and T . After decomposition, the number of non-zero diagonal elements in the linear transformations is significantly reduced, resulting in a notable reduction in the number of keys required in the outer loop while preserving the integrity of hoisting. Additionally, the computation speed of the Z, T transformation improves as the number of keys decreases.

4.2 Simple Key Substitution Method

We begin by presenting a simple key substitution method, which is essentially a general key substitution strategy applied to row and column transformations. By performing hoisting rotations on a single ciphertext with any set of rotation steps of equal arithmetic progression ($k = a \cdot q$, where $a \in (0, d) \cap \mathbb{Z}$), it is possible to achieve the same effect using a reduced set of rotation keys with steps $k = a \cdot q$ ($a \in (0, d_1) \cap \mathbb{Z}$ and $d_1 < d$). When applying this strategy to the ciphertext computed in the BSGS algorithm's memory loop precomputation, an additional cost of n_1/n'_1 Decompose and ModDown operations is incurred to reduce the number of rotation keys from n_1 to n'_1 .

For example, consider $Z\mathbf{x}$ with $n = 128$, where $n_{Z1} = 16$ and $n_{Z2} = 8$ represent the number of iterations in the inner and outer loops, respectively. Initially, it requires 30 keys ($16 - 1 + 8 \times 2 - 1$). By applying the simple key substitution method, the number of keys can be reduced to 23 at the cost of one Decompose and ModDown operation.

However, the simple key substitution method has limited effectiveness in scenarios with low computational space requirements. This is because a lower computational space implies fewer iterations in the inner loop, which leads to an increase in the number of outer loop iterations and the corresponding required keys. As the simple key substitution method cannot be applied to the outer loop, the benefits of saving keys in the inner loop diminish. Continuing with the previous example, if we attempt to reduce n_{Z1} by half to decrease the space requirements, n_{Z2} will correspondingly double. In this case, 38 keys would be required ($8 - 1 + 16 \times 2 - 1$), and the simple key substitution method can only reduce it to 34 keys at the same cost. Therefore, we still need to find a method that can balance both low intermediate space requirements and a reduced number of rotation keys.

4.3 Decomposition of Diagonal Vector Convergence for Specific Permutation Matrix

In equation (3), the number of outer loop iterations is essentially determined by the number of non-zero diagonal vectors in the linear transformation matrices. By reducing the number of non-zero diagonal

vectors required for the linear transformations, we can simultaneously decrease the runtime memory footprint and the number of rotation keys. Hereafter, we will decompose the linear transformations of Z and T to achieve a reduction in the number of non-zero diagonal vectors.

Definition 1 establishes a correspondence between the indices of diagonal vectors and elements in the additive group, determining the arithmetic rules between subsequent indices. The subsequent indices belonging to $(\mathbb{Z}/n\mathbb{Z}, +)$ are represented using representatives from both the intervals $(-n/2, n/2)$ and $[0, n - 1]$. Definition 2 introduces the Diagonal Vector Convergence Decomposition, emphasizing a decreasing trend in the number of non-zero diagonal vector types after the matrix is decomposed. We focus on a specific type of Diagonal Vector Convergence, which decomposes a permutation matrix A into Boolean matrices with no repeated 1 values in each row and column. In Definition 3, we provide two methods for locating coordinates in square matrices: one based on row and column indices and the other based on diagonal and row indices. Theorem 2 reveals the connection between row, column, and diagonal indices when performing the decomposition of Boolean matrices. It is of crucial importance for our subsequent design. Definition 4 introduces a term, based on the pattern revealed in Theorem 2, for decomposing k diagonal vectors of matrix A into the k_2 th diagonal of the left matrix A_2 and the k_1 th diagonal of the right matrix A_1 . This term explains how the values of the diagonals in A_1 and A_2 should be set for a given diagonal vector in A , and we will use this term later on. Next, we will individually design specific Diagonal Vector Convergence methods for the linear transformations Z and T to reduce their number of non-zero diagonal vectors.

Definition 1. For any $n \times n$ square matrix, we represent its column indices, row indices, and diagonal vector indices using the additive group $(\mathbb{Z}/n\mathbb{Z}, +)$, where the indices of the diagonal vectors are defined based on the column indices of the elements in the first row of the matrix.

Definition 2. We refer to a matrix decomposition as a **diagonal vector convergence decomposition** when it expresses a square matrix as a product and sum of a series of matrices, and the total number of distinct diagonal vector indices in these matrices is smaller than the number of distinct diagonal vector indices in the original matrix.

Definition 3. For an $n \times n$ square matrix, the element located at row i and column j possesses a normal coordinate $N(i, j) \in (\mathbb{Z}/n\mathbb{Z})^2$, and a diagonal coordinate $D(k, l) \in (\mathbb{Z}/n\mathbb{Z})^2$. Thus, there exists a mapping $f : (\mathbb{Z}/n\mathbb{Z})^2 \rightarrow (\mathbb{Z}/n\mathbb{Z})^2$ that transforms a normal coordinate to a diagonal coordinates:

$$\begin{aligned} f(N(i, j)) &= D(j - i, i) \\ f^{-1}(D(k, l)) &= N(l, k + l) \end{aligned} \quad (5)$$

We denote the symbol $A_{N(i, j)}$ to represent the element of A located at the normal coordinate $N(i, j)$, and $A_{D(k, l)}$ to represent the element of A located at the diagonal coordinate $D(k, l)$.

Theorem 2. According to Definitions 1, 2, and 3, let A be a boolean matrix (i.e., a matrix containing only 0 or 1 values) that can be decomposed into $A = A_2 A_1$, where A_1 and A_2 are both boolean matrices. For any 1 element $A_{N(i, j)}$ in A , there exists a unique index $0 \leq a < n$ in A_1 and A_2 such that $A_{1N(a, j)}$ and $A_{2N(i, a)}$ are both 1. Furthermore, considering $D(k, i) = f(N(i, j))$, $D(k_1, a) = f(N(a, j))$, and $D(k_2, i) = f(N(i, a))$, we have $k_1 + k_2 = k$.

Definition 4. For a boolean matrix A , A_1 , and A_2 of size $n \times n$, decomposing the k th diagonal of A onto the k_1 th diagonal of the right matrix A_1 , and the k_2 th diagonal of the left matrix A_2 refers to the following process: For each 1 element $A_{D(k, l)}$ in the k th diagonal, set $A_{1D(k_1, k+l-k_1 \bmod n)}$ to 1, which corresponds to the element on the k_1 th diagonal with the same column index as k . Also, set $A_{2D(k_2, l)}$ to 1, which corresponds to the element on the k_2 th diagonal with the same row index as k . Here, $k_1 + k_2 = k$.

Decomposition of Linear Transformation Z The value of the ℓ -th component in the k -th non-zero diagonal vector $\mathbf{z}_k[\ell]$ can be expressed as (all operations below involving non-zero diagonal vector indices are assumed to be in $(\mathbb{Z}/n^2\mathbb{Z}, +)$):

$$\mathbf{z}_k[\ell] = \begin{cases} 1, & \text{if } k \geq 0 \text{ and } 0 \leq \ell - n \cdot k < (n - k); \\ 1, & \text{if } k < 0 \text{ and } -k \leq \ell - (n + k) \cdot n < n; \\ 0, & \text{otherwise.} \end{cases} \quad (6)$$

We observe that the 1 values of Z are symmetrically distributed on both sides of the 0th diagonal vector. They can be divided into n submatrices of size $n \times n$, each having the 0th diagonal vector of Z as its own 0th diagonal vector. These submatrices do not overlap with each other. We can decompose Z by decomposing these submatrices. For any submatrix S , S always contains n elements with a value of 1, and these elements are always located on the two diagonals k_1 and k_2 of Z which have the following characteristic: $|[k_1]n^2| \leq \lceil \frac{n-1}{2} \rceil$ and $|[k_2]n^2| > \lceil \frac{n-1}{2} \rceil$. Furthermore, if we denote S_i , $0 \leq i < n$, as the n submatrices of diagonals of Z , then the 1 values in S_i always fill the diagonals i and $i - n \bmod n^2$ of Z . To perform a diagonal convergence decomposition of Z , we first need to determine the desired number of diagonals. Since the non-zero diagonal indices of Z form an arithmetic progression with a common difference of 1, we reach a consensus here: if the maximum absolute value of the expected non-zero diagonal indices (within the remaining range $(-n^2 + 1, n^2 - 1)$) is n' , then it is equivalent to having all non-zero diagonal vectors of the resulting matrices belong to the set $[-n', n'] \cap \mathbb{Z}$. The decomposition of Z will always follow the format:

1. Divide Z into the format $Z = Z_1 + Z_2$, where Z_1 is the matrix containing all non-zero diagonal vectors of Z with absolute values greater than $\lceil \frac{n-1}{2} \rceil$ (centralized modulo n^2), and Z_2 is the matrix containing all non-zero diagonal vectors of Z with absolute values less than or equal to $\lceil \frac{n-1}{2} \rceil$. This step ensures that each submatrix of Z_1 and Z_2 has at most one non-zero diagonal vector, and each non-zero diagonal vector's 1-value components belong to a specific submatrix.
2. Decompose both Z_1 and Z_2 using Algorithm 5 into $\lceil \frac{n-1}{n'} \rceil$ and $\lceil \frac{\lceil \frac{n-1}{2} \rceil}{n'} \rceil$ matrix products, respectively, as follows:

$$Z = \prod_{i=1}^{\lceil \frac{n-1}{n'} \rceil} Z_{1i} + \prod_{i=1}^{\lceil \frac{\lceil \frac{n-1}{2} \rceil}{n'} \rceil} Z_{2i} \quad (7)$$

The decomposed expressions of both products have the same characteristic: only the rightmost matrix has non-zero diagonal vectors with indices belonging to the interval $[-n' + 1, n' - 1] \cap \mathbb{Z}$, while the remaining matrices have only non-zero diagonal vectors with indices $-n', n', 0$. Therefore, the dominant complexity at this point lies in the two linear transformations $Z_{1\lceil \frac{n-1}{n'} \rceil}$ and $Z_{2\lceil \frac{\lceil \frac{n-1}{2} \rceil}{n'} \rceil}$ on the right-hand side. They still preserve a property of arithmetic progression and can share the same set of inner-loop pre-rotations of ciphertext.

Decomposition of Linear Transformation T Transformation T consists of n non-zero diagonal vectors, whose indices are $\{k \cdot n | 0 \leq k < n\}$. For the $k \cdot n$ -th non-zero diagonal vector \mathbf{t}_{kn} of T , the value of its ℓ -th component $\mathbf{t}_{kn}[\ell]$ can be expressed as:

$$\mathbf{t}_{kn}[\ell] = \begin{cases} 1, & \text{if } \ell \in \{k + n \cdot i | 0 \leq i < n\}; \\ 0, & \text{otherwise.} \end{cases} \quad (8)$$

Let the maximum absolute value of the desired non-zero diagonal index be $n \cdot n'$. This implies that all non-zero diagonal vectors in the decomposition result belong to the set $[0, n' \cdot n]$. We will decompose T into the following form using Algorithm 6:

$$T = \prod_{i=1}^{\lceil \frac{n-1}{n'} \rceil} T_i \quad (9)$$

The non-zero diagonals of T have a consistent spacing between the elements with a value of 1, but their starting positions differ. For the in -th non-zero diagonal, where $0 \leq i < (n-1)$, the first element with a value of 1 starts at position i . This structured, yet not compact, arrangement allows us to easily decompose T in the desired manner. The proof for the correctness of Algorithm 6 is given in Appendix (see theorem 7). Similar to the decomposition of Z , the resulting cumulative product in Algorithm 6 has only the rightmost matrix with non-zero diagonals in the interval $[0, (n' - 1)n] \cap \mathbb{Z}$, while all other left matrices have only non-zero diagonals at indices $n'n$ and 0. This implies that the complexity of the cumulative product is dominated by the complexity of the rightmost linear transformation, whose diagonal indices belong to a smaller range compared to the original approach.

Algorithm 5 Diagonal Convergence Decompose for LinTrans Z (DCDforZ)

Input: Matrix Z with size $n^2 \times n^2$, the maximum non-zero diagonal index $n - 1$, and the target maximum non-zero diagonal index n' .

Output: Decomposed matrices $Z_i | Z = \prod_{i=1}^{\lceil \frac{n}{n'} \rceil} Z_i$

```
1: for  $i = 1$  to  $\lceil \frac{n}{n'} \rceil - 1$  do
2:   Initialize matrices  $Z^{(0)}$  and  $Z^{(1)}$  as zero matrices.
3:   for each non-zero diagonal vector  $|[k]_{n^2}| \geq n'$  in  $Z$  do
4:     Decompose the vector to the  $n'$ -th non-zero diagonal vector of the left matrix  $Z^{(0)}$  and the
        $(k - \text{sign}([k]_{n^2}) \cdot n')$ -th diagonal of the right matrix  $Z^{(1)}$ .
5:   end for
6:   for each non-zero diagonal vector  $[k]_{n^2} < n'$  in  $Z$  do
7:     Decompose the vector to the 0-th non-zero diagonal vector of the left matrix  $Z^{(0)}$  and the
        $k$ -th diagonal of the right matrix  $Z^{(1)}$ .
8:   end for
9:   (At this point,  $Z = Z^{(0)} Z^{(1)}$ )
10:  if this is not the last iteration then
11:     $Z_i \leftarrow Z^{(0)}$ ,  $Z \leftarrow Z^{(1)}$ 
12:  else
13:     $Z_i \leftarrow Z^{(0)}$ ,  $Z_{i+1} \leftarrow Z^{(1)}$ 
14:  end if
15: end for
16: return  $\{Z_i\}$ 
```

Algorithm 6 Diagonal Convergence Decompose for LinTrans T (DCDforT)

Input: Matrix T with size $n^2 \times n^2$, the maximum non-zero diagonal index $(n - 1)n$, and the target maximum non-zero diagonal index $n'n$.

Output: Decomposed matrices $\{T_i | T = \prod_{i=1}^{\lceil \frac{n-1}{n'} \rceil} T_i\}$

```
1: for  $i = 1$  to  $\lceil \frac{n}{n'} \rceil - 1$  do
2:   Initialize  $T^{(0)}$  and  $T^{(1)}$  as zero matrices.
3:   Traverse the  $i \cdot n$ -th non-zero diagonal of  $T$ , where  $0 \leq i \leq n'$ , and decompose it onto the 0th
       diagonal of the left matrix  $T^{(0)}$  and the  $i \cdot n$ -th diagonal of the right matrix  $T^{(1)}$ .
4:   Traverse the  $i \cdot n$ -th non-zero diagonal of  $T$ , where  $n' < i \leq (n - 1)$ , and decompose it onto the
        $n' \cdot n$ -th diagonal of the left matrix  $T^{(0)}$  and the  $(i - n') \cdot n$ -th diagonal of the right matrix  $T^{(1)}$ .
5:   (At this point,  $T = T^{(0)} T^{(1)}$ )
6:   if this is not the last iteration then
7:      $T_i \leftarrow T^{(0)}$ ,  $T \leftarrow T^{(1)}$ 
8:   else
9:      $T_i \leftarrow T^{(0)}$ ,  $T_{i+1} \leftarrow T^{(1)}$ 
10:  end if
11: end for
12: return  $\{T_i\}$ 
```

We compared the rotation key count and computational complexity (in terms of internal rotation operations) of the diagonal convergence decomposition, simple key substitution method, and the dh-BSGS algorithm without any key simplification strategy for the Z and T transformations in Table (4.3).

More specific experimental data is provided in Table (4.3), using the Z and T transformations in a 128 x 128 matrix multiplication as an example. It shows the key size, maximum runtime space, and execution time for different internal loop counts and diagonal convergence decompositions with different expected maximum non-zero diagonal indexes. It should be noted that the internal loop count (n_1) is linearly related to the maximum runtime space of the linear transformation. From the table, we can observe that our diagonal convergence decomposition reduces the number of rotation operations required for the linear transformation as the maximum diagonal index of the decomposed matrices decreases. When maintaining a low internal loop count (e.g., $n_1 = 8$), the reduction in rotation key count is more than half, allowing for more instances of linear transformations to be parallelized within a fixed space. As a result, our approach achieves higher efficiency, lower runtime space requirements, and reduced rotation key count. Finally, we provide the complete process of ciphertext decomposition matrix multiplication with diagonal convergence decomposition in Algorithm 7, omitting the internal optimization details such as double-hoisting and hoisting, and presenting a high-level illustrative flow.

Scheme	LT	MaxDiagNo.	MinRotKeys	Complexity(Rotations)
dh-BSGS	Z	$n - 1$	$n_1 + 2n_2 - 2$	$(n_1 + 2n_2) \cdot (MS + Pm) + (2n_2 + 1) \cdot (Dp + MD)$
SmpKeySub	Z	$n - 1$	$n'_1 + 2n_2 - 2$	$(n_1 + 2n_2) \cdot (MS + Pm) + (2n_2 + 1 + n_1/n'_1) \cdot (Dp + MD)$
DCDmp	Z	m	$n_1 + 2m/n_1 - 1$	$(n_1 + 4m/n_1 + 3n/m - 4) \cdot (MS + Pm) + (4m/n_1 + 1 + 3n/m - 4) \cdot (Dp + MD)$
dh-BSGS	T	$(n - 1) \cdot n$	$n_1 + n_2 - 2$	$(n_1 + n_2) \cdot (MS + Pm) + (n_2 + 1) \cdot (Dp + MD)$
SmpKeySub	T	$(n - 1) \cdot n$	$n'_1 + n_2 - 2$	$(n_1 + n_2) \cdot (MS + Pm) + (n_2 + 1 + n_1/n'_1) \cdot (Dp + MD)$
DCDmp	T	$m \cdot n$	$n_1 + m/n_1 - 1$	$(n_1 + m/n_1 + n/m - 1) \cdot (MS + Pm) + (m/n_1 + n/m) \cdot (MS + Pm)$

Table 2: Rotation Complexity and Minimal Rtk Number Comparison of LinTrans Z, T among original double-hoisting BSGS(dh-BSGS), dh-BSGS with Simple Key Substitution(SmpKeySub) and dh-BSGS with Diagonal Vector Convergence Decomposition(DCDmp)

Scheme	Matrix	n_1	MaxDiagNo.	RotKeySpace(MB)	run-timeSpace(MB)	time(s)	Depth
dh-BSGS	Z	8	127	1755	63	2.860	1
DCDmp	Z	8	32	720	63	1.954	4
dh-Ours	Z	8	16	540	63	1.707	8
DCDmp	Z	16	127	1395	135	1.859	1
dh-Ours	Z	16	32	900	135	1.479	4
DCDmp	T	8	127 · 128	1035	63	1.628	1
dh-Ours	T	8	64 · 128	720	63	1.106	2
DCDmp	T	8	32 · 128	540	63	0.811	4
dh-BSGS	T	16	127 · 128	1035	135	1.028	1
DCDmp	T	16	64 · 128	900	135	0.784	2
DCDmp	T	16	32 · 128	810	135	0.750	4

Table 3: Run-time performance Comparison of LinTrans Z, T between original double-hoisting BSGS(dh-BSGS) and our Diagonal Convergence Decomposed scheme(DCDmp). The data is retrieved under a set of homomorphic encryption parameters: $\log QP = 760$, $\log N = 15$, $\log(\text{Slots}) = 14$

Algorithm 7 Matrix Multiplication using Diagonal Convergence Decomposition (DCDmp-MatrixMult)

Input: ciphertexts for matrix A, B with size $n \times n$: $\text{ct}(A), \text{ct}(B)$; expected maximum non-zero diagonal index for Z : n'_Z expected maximum non-zero diagonal index for T : $n \cdot n'_T$

Output: $\text{ct}(AB)$

```

1:  $\{Z_{1i}\}, \{Z_{2i}\}, Z_3 \leftarrow \text{DCDforZ}(n^2, n'_Z)$ 
2:  $\{T_i\} \leftarrow \text{DCDforT}(n^2, n \cdot n'_T)$ 
3:  $\text{ct}(A_1), \text{ct}(A_2) \leftarrow \text{ct}(A)$ 
4:  $\text{ct}(B^{(0)}) \leftarrow \text{ct}(B)$ 
5: for  $Z_{1i}$  in  $\{Z_{1i}\}$  do
6:    $\text{ct}(A_1) \leftarrow \text{LinTrans}(\text{ct}(A_1), Z_{1i})$ 
7: end for
8: for  $Z_{2i}$  in  $\{Z_{2i}\}$  do
9:    $\text{ct}(A_2) \leftarrow \text{LinTrans}(\text{ct}(A_2), Z_{2i})$ 
10: end for
11:  $\text{ct}(A_3) \leftarrow \text{LinTrans}(\text{ct}(A), Z_3)$ 
12: for  $T_i$  in  $\{T_i\}$  do
13:    $\text{ct}(B^{(0)}) \leftarrow \text{LinTrans}(\text{ct}(B^{(0)}), T_i)$ 
14: end for
15:  $\text{ct}(AB) \leftarrow \text{Mul}(\text{ct}(A^{(0)}), \text{ct}(B^{(0)}))$ 
16: for  $1 \leq k < n$  do
17:    $\text{ct}(A^{(k)}) \leftarrow \text{LinTrans}(\text{ct}(A^{(k-1)}), C^k)$ 
18:    $\text{ct}(B^{(k)}) \leftarrow \text{LinTrans}(\text{ct}(B^{(k-1)}), R^k)$ 
19:    $\text{ct}(AB^{(k)}) \leftarrow \text{Mul}(\text{ct}(A^{(k)}), \text{ct}(B^{(k)}))$ 
20:    $\text{ct}(AB) \leftarrow \text{Add}(\text{ct}(AB^{(k-1)}), \text{ct}(AB))$ 
21: end for
22: return  $\text{ct}(AB)$ 

```

5 Homomorphic Covariance Matrix Computation for Large Datasets

In the previous section, we presented an optimization for matrix multiplication. In this section, we will first introduce a method for ciphertext packing of large datasets, enabling seamless execution of matrix multiplication on encrypted data. Next, by leveraging homomorphic matrix multiplication and other homomorphic operations, we propose an algorithm that efficiently computes the covariance matrix of a dataset using only encrypted dataset elements.

5.1 Ciphertext Packing

Let us consider a dataset, denoted as X , consisting of tens of thousands of rows of samples/records, with each sample having hundreds of features. We focus on how to pack the dataset into ciphertexts, maximizing space utilization while facilitating vector and matrix operations. Let X be an $s \times t$ matrix, where s represents the number of samples and t represents the number of features. Our strategy involves partitioning X into square matrices, as this facilitates the execution of homomorphic square matrix operations. Therefore, we consider schemes where the number of message slots is $n^2 = N/2^i$, where $1 \leq i < \log(N)$, allowing us to treat the ciphertext as an $n \times n$ matrix. We will divide the features into k partitions, where $k = \lceil \frac{t}{n} \rceil$. Each ciphertext will contain one partition of features from n samples/records, meaning that k ciphertexts will collectively represent all the feature values of n samples. Note that t is not always divisible by n , so zero-padding is necessary. Two possible methods for padding are as follows:

1. The first $k - 1$ ciphertexts will each contain different sets of n feature values, while the last ciphertext will contain the actual feature values of $t - k \cdot n$ samples, padded with zero values. This approach expands the feature count from t to $k \cdot n$ and treats each ciphertext as an $n \times n$ matrix representing n samples with n features.

2. The first $k - 1$ ciphertexts are padded with $p = \lfloor (t - k \cdot n) / k \rfloor$ zero-valued features, and only store $n - p$ valid features. This approach allows each ciphertext to be viewed as an $n \times (n - p)$ matrix, taking advantage of some possible optimizations for non-square matrix multiplication while still enabling operations on square matrices.

In summary, we require $\lceil s/n \rceil \cdot k$ ciphertexts to pack the entire dataset X .

5.2 Homomorphic Covariance Matrix Computation for Large Datasets

We present a method for computing the covariance matrix of an encrypted dataset. Let us assume that we have partitioned X into $\lceil s/n \rceil \cdot k$ ciphertexts, with each ciphertext representing an $n \times n$ submatrix of X . We denote X_i as the i -th column submatrix of X , where $0 \leq i < k$. We also define $X_i[\ell]$ as the ℓ -th submatrix of X_i . We represent the ciphertext of $X_i[\ell]$ as $\text{ct}(X_i[\ell])$.

Next, we compute the covariance matrix Cov based on these submatrices. If the dataset is not centered, we first need to calculate the mean 'vector' μ of the dataset. In fact, μ is represented by k submatrices, where each column of a submatrix has the same value, representing the mean of the corresponding feature. We use $\mu[i]$ to denote the i -th submatrix of the mean 'vector', where $0 \leq i < k$. This requires the use of a row aggregation function, to sum up the rows within a submatrix:

$$\mu[i] = \text{Aggregate} \left(\sum_{0 \leq \ell < \lceil s/n \rceil} X_i[\ell]; 0 \right) \quad (10)$$

where $\text{Aggregate}(X; \text{axis})$, $a \in \{1, 0\}$ represents aggregating the matrix X by columns ($\text{axis} = 1$) or by rows ($\text{axis} = 0$). The detailed process is provided in Algorithm 8.

Algorithm 8 Aggregate

Input: $\text{ct}(X)$ a ciphertext of a matrix, aggregation axis axis , matrix dimensions row and col

Output: $\text{ct}(\text{Aggregate}(X; \text{axis}))$

```

1:  $\text{ct}(A) \leftarrow \text{ct}(X)$ 
2: if  $\text{axis} == 0$  then
3:   for  $i \leftarrow \text{col}; i < \text{row} \cdot \text{col}; i = (i << 1)$  do
4:      $\text{ct}(A) \leftarrow \text{Add}(\text{Rot}(\text{ct}(A); i), \text{ct}(A))$ 
5:   end for
6: end if
7: if  $\text{axis} == 1$  then
8:   for  $i \leftarrow 1; i < \text{col}; i = (i << 1)$  do
9:      $\text{ct}(A) \leftarrow \text{Add}(\text{Rot}(\text{ct}(A); i), \text{ct}(A))$ 
10:  end for
11:  $\text{ct}(A) \leftarrow \text{Mult}(\text{ct}(A), \text{pt}(M))$ , where  $M$  is a mask matrix with the same dimensions as  $X$ , except
    for the first column elements which are all 1 and other elements are 0
12: for  $i := -1; i > -\text{col}; i = (i << 1)$  do
13:    $\text{ct}(A) \leftarrow \text{Add}(\text{Rot}(\text{ct}(A); i), \text{ct}(A))$ 
14: end for
15: end if
16: return  $\text{ct}(A)$ 
```

Theorem 3. *The multiplication depth of Algorithm 8 is at most 1, and the time complexity is dominated by the number of rotations, which is $O(\log(\text{row}))$ or $O(\log(\text{col}))$.*

Furthermore, we compute $\mu^T \mu$. Since each $\mu[i]$ contains n copies of the feature means, this step can be accomplished by a simple transpose and coordinate-wise multiplication:

$$\mu^T \mu[i] = \mu[j]^T \odot \mu[i] \quad (11)$$

Next, we iterate through each column submatrix X_i of X and traverse the k column submatrices X_j , $0 \leq j < k$ to compute:

$$X^T X[i] = \sum_{0 \leq \ell < \lceil s/n \rceil} X_j[\ell]^T X_i[\ell] \quad (12)$$

Here, $X^T X$ is of size $k \times k$ (measured in submatrices), and the above equation can be interpreted as the inner product operation between two column submatrices of the covariance matrix. If X is already centered, then $X^T X$ represents the covariance matrix. Otherwise, we need to subtract $\mu^T \mu$. It is worth noting that directly computing the covariance matrix using the above equation is not the most efficient implementation. We can optimize it in the following two ways:

1. Considering that in Section 3, we mentioned that when multiplying a matrix A with a series of matrices B_1, B_2, \dots , we can reduce more than half of the matrix multiplication overhead by storing $C^k Z \mathbf{a} | k = 0, \dots, n$. Therefore, for a given j , we can perform the inner product operations of the k column submatrices in parallel: $\sum_{0 \leq \ell < \lceil s/n \rceil} X_j[\ell]^T X_i[\ell], 0 \leq i < k$, and save nearly half of the computation time by storing $\{C^k Z \text{ct}(X_j[\ell]^T) | 0 \leq \ell < \lceil s/n \rceil\}$.
2. Based on the fact that the covariance matrix is a symmetric matrix, it suffices to calculate the results of one side of the diagonal and transpose them to obtain the results for the other side, saving us half of the covariance computation time.

The calculation of the entire encrypted covariance matrix is given in Algorithm 9. Since optimization 1 involves restructuring the internal computation order of matrix multiplication, it is not explicitly shown in Algorithm 9, but a slight restructuring of the fourth step in the first loop is sufficient to implement it.

Algorithm 9 Covariance Matrix Computation (CovMtrx)

Input: Partitioned and encrypted dataset $\text{ct}(X_j[\ell]) | 0 \leq j < k, 0 \leq \ell < \lceil s/n \rceil$, maximum diagonal index n_Z for transformation Z , maximum diagonal index n_T for transformation T

Output: Partitioned ciphertext covariance matrix $\text{ct}(\text{Cov}_i[j]) | 0 \leq i, j < k$

```

1: for  $0 \leq j < k$  do
2:   Take  $\text{ct}(X_j[\ell]), 0 \leq \ell < \lceil s/n \rceil, \text{ct}(\mu[j]) \leftarrow \sum_{0 \leq \ell < \lceil s/n \rceil} X_i[\ell]$ 
3:   for  $n \leq t < n^2$  do
4:      $\text{ct}(\mu[j]) \leftarrow \text{Add}(\text{ct}(\mu[j]), \text{Rot}(\text{ct}(\mu[j]); t))$ 
5:      $t \leftarrow t + 1$ 
6:   end for
7:   Compute  $\text{ct}(X_j[\ell]^T) \leftarrow \text{LinTrans}(\text{ct}(X_j[\ell]), \text{TP})$  in parallel for  $0 \leq \ell < \lceil s/n \rceil$ 
8:   for  $0 \leq i < j$  do
9:     Compute  $\text{ct}(X_j[\ell]^T X_i[\ell]) \leftarrow \text{DMtrxMul}(\text{ct}(X_j[\ell]^T), \text{ct}(X_i[\ell]), n, n_Z, n_T)$  in parallel for  $0 \leq \ell < \lceil s/n \rceil$ 
10:    Aggregate the parallel computation results to obtain  $\text{ct}(X^T X_i[j]) \leftarrow \sum_{0 \leq \ell < k} \text{ct}(X_j[\ell]^T X_i[\ell])$ 
11:  end for
12: end for
13: for  $0 \leq j < k$  do
14:   for  $j \leq i < k$  do
15:     $\text{ct}(X^T X_i[j]) \leftarrow \text{LinTrans}(\text{ct}(X^T X_j[i]), \text{TP})$ 
16:   end for
17: end for
18: for  $0 \leq j < k$  do
19:    $\text{ct}(\mu[j]^T) \leftarrow \text{LinTrans}(\text{ct}(\mu[j]), T)$ 
20:   for  $0 \leq i < k$  do
21:     $\text{ct}(\mu^T \mu_i[j]) \leftarrow \text{Mul}(\text{ct}(\mu[j]^T), \text{ct}(\mu[i]))$ 
22:     $\text{ct}(\text{Cov}_i[j]) \leftarrow \text{Add}(\text{ct}(X^T X_i[j]), \text{ct}(-\mu^T \mu_i[j]))$ 
23:   end for
24: end for
25: return  $\{\text{ct}(\text{Cov}_i[j]) | 0 \leq i, j < k\}$ 

```

Theorem 4. The multiplication depth of Algorithm 9 is $2 + \max(\lceil \frac{(n-1)}{n_Z} \rceil, \lceil \frac{(n-1)*n}{n_T} \rceil) + 2$, and the time complexity is dominated by the number of matrix multiplications, which is $O(\frac{1}{2}k^2 \cdot \lceil s/n \rceil)$.

6 Privacy-Preserving PCA using Homomorphic PowerMethod

In this section, we first present the homomorphic evaluation circuit of the PowerMethod algorithm in the first subsection. In the second subsection, we demonstrate the process of performing privacy-preserving PCA utilizing our homomorphic PowerMethod circuit.

6.1 Homomorphic PowerMethod Circuit

We divide the demonstration of the homomorphic PowerMethod into two pivotal components: the continuous transformation of the covariance matrix and the normalization of the approximate eigenvector. In addition, the computation of the eigenvalue corresponding to the eigenvector will be presented subsequently.

6.1.1 Covariance Matrix Transformation

Since the covariance matrix is typically a large matrix composed of multiple submatrices (i.e., multiple ciphertexts), we design a method for the linear transformation of large matrices. For a column vector (or row vector) with the same number of columns (or rows) as the covariance matrix, we extend it into a column (or row) of submatrices using the following approach:

1. Divide the vector evenly into k segments, where each segment has the same length as the number of rows (or columns) in a submatrix.
2. horizontally (or vertically) replicate these k segments of column vectors (or row vectors) n times to construct k submatrices.

The continuous linear transformation in the PowerMethod will alternate between the horizontally replicated vector matrices and the vertically replicated vector matrices. Let's examine how the matrix representations of the two types of vectors are applied in the linear transformation with the covariance matrix. Let V_{t-1} be a row of sub-matrices used to represent a vector. If it is constructed by horizontally replicating column vectors, then for any $0 \leq i < k$:

$$\begin{aligned} V_t[i] &= \text{Aggregate} \left(\sum_{0 \leq j < k} (\text{Cov}_j[i] \odot V_{t-1}[j]^T)^T; 0 \right) \\ &= \text{Aggregate} \left(\sum_{0 \leq j < k} \text{Cov}_j[i]^T \odot V_{t-1}[j]; 0 \right) \end{aligned} \quad (13)$$

Here, $V_t[i]$, $0 \leq i < k$, now have the same number of rows. If we consider any row in $[V_t[0] | V_t[1] | \dots | V_t[k-1]]$ as the row vector \mathbf{v}_t^T , and any column in $(V_{t-1}[0] | V_{t-1}[1] | \dots | V_{t-1}[k-1])$ as the column vector \mathbf{v}_{t-1} , we have $\mathbf{v}_t^T = (\text{Cov} \cdot \mathbf{v}_{t-1})^T$. Similarly, if V_{t-1} is constructed by vertically replicating row vectors, then for any $0 \leq i < k$:

$$V_t[i] = \text{Aggregate} \left(\sum_{0 \leq j < k} V_{t-1}[j] \odot \text{Cov}_i[j]^T; 1 \right) \quad (14)$$

Where $V_t[i]$, $0 \leq i < k$ will have the same number of columns. If we consider any column in $(V_t[0] | V_t[1] | \dots | V_t[k-1])$ as the column vector \mathbf{v}_t , and any row in $[V_{t-1}[0] | V_{t-1}[1] | \dots | V_{t-1}[k-1]]$ as the row vector \mathbf{v}_{t-1}^T , we have $\mathbf{v}_t = (\text{Cov} \cdot \mathbf{v}_{t-1}) = (\mathbf{v}_{t-1}^T \cdot \text{Cov})$. This equation holds because the covariance matrix Cov is symmetric, i.e., $\text{Cov}^T = \text{Cov}$ and $\text{Cov}_j[i]^T = \text{Cov}_i[j]$. From this, we can see that we can always perform the continuous linear transformation of the covariance matrix with Hadamard multiplication, summation, aggregation, and intermediate vectors alternating between row and column form.

At the onset of the PowerMethod iteration, we initially select a random initial row vector, denoted as v_0 , of dimension d . Subsequently, we vertically replicate (Replicate) it d times, forming a series of submatrices referred to as V_0 . The i th submatrix within this row-wise arrangement is denoted as $V_0[i]$. Throughout the PowerMethod iteration, we utilize the notation V_t to represent the series of

eigenvector matrices obtained at the t th iteration. Consequently, the computation of the eigenvector matrix $V_t[i]$ in the t th iteration of the PowerMethod can be expressed as follows:

$$V_t[i] = \text{Aggregate} \left(\sum_{0 \leq j < k} V_{t-1}[j] \odot \text{Cov}_j[i]; t+1 \bmod 2 \right) \cdot (t+1 \bmod 2) + \text{Aggregate} \left(\sum_{0 \leq j < k} V_{t-1}[j] \odot \text{Cov}_i[j]; t \bmod 2 \right) \cdot (t \bmod 2) \quad (15)$$

6.1.2 Vector normalisation

In plaintext computation scenarios, it is customary to scale the approximate eigenvector results obtained in each round of the PowerMethod iteration and employ the scaled results as inputs for the next iteration. This is done to prevent the length of the eigenvectors from continually increasing or decreasing, which could lead to overflow. It is worth noting that the scaling performed during the iteration does not affect the convergence speed of the iteration. In the context of homomorphic encryption, where the actual values of the eigenvectors are not visible, it is difficult to scale the approximate eigenvectors using a fixed (set of) constant factors. Therefore, we adopt a normalization scaling approach, which ensures that the norm of the eigenvectors is kept within a reasonable range after each scaling. Given that current homomorphic encryption schemes generally do not support the evaluation of non-polynomial functions, achieving normalization necessitates approximating the InvSRT function within a certain range using an iterative approach. Based on existing research on the approximation of the InvSRT function using iterative algorithms in the homomorphic setting, we have summarized the following factors that significantly influence the accuracy of the approximation:

1. Number of iterations: The more iterations performed, the closer the approximation of the InvSqrt function will be to the exact value.
2. Initial estimate: Given a fixed number of iterations, a closer initial approximation to the exact value yields more accurate results from the iterative algorithm. Conversely, an initial estimate that deviates significantly from the exact value may prevent the iterative algorithm from converging. Since the function $\frac{1}{\sqrt{x}}$ exhibits significant changes in slope on both sides of 1, resembling an "L" shape, determining an initial approximation that simultaneously approximates the exact value on both sides of 1 using a simple function (such as a low-degree polynomial) may be insufficient. However, constructing an initial approximation evaluation method that closely approximates the exact value on both sides of the evaluation interval can itself be a complex task. For example, approaches such as the piecewise function used in [Pan22] or the rational polynomial function discussed in [QX] yield initial estimates that are closer to the exact value. However, even these functions require an iterative approximation in the homomorphic setting.

Faced with the aforementioned facts, our first step is to determine the upper bound of the norm of the approximate eigenvectors in order to establish the evaluation range for the square root reciprocal iteration algorithm. Subsequently, we propose a Lazy Normalization strategy for scaling the approximate eigenvectors. This strategy tolerates imprecise outputs of the square root reciprocal iteration algorithm within the interval (0,1] during some rounds of the PowerMethod. However, it aims to achieve highly accurate outputs in the final iteration to ensure that the resulting eigenvectors are normalized.

Estimating the Upper Bound of the Norm: After the dataset has undergone normalization and centering, let's assume that each eigenvalue is bounded within $b > 0$. Consequently, for each element in the covariance matrix Cov, we have the bound $|\text{Cov}_{ij}| = \frac{1}{n} |\langle \mathbf{x}_i, \mathbf{x}_j \rangle| \leq b^2$, where $\mathbf{x}_i, 0 \leq i < d$ represents the vector composed of the i -th feature values of all samples in the dataset. Therefore, the Euclidean norm of vector Cov_i is bounded by $\|\text{Cov}_i\|_2 \leq \sqrt{b^4 \cdot d}$. With this information, we can roughly estimate the upper bounds of various norms for the matrix transformation $\mathbf{y} = \text{Cov} \cdot \mathbf{v}$. For instance, assuming that the Euclidean norm of the input eigenvector \mathbf{v} during the first iteration does

not exceed c , applying the Cauchy-Schwarz inequality, the Euclidean norm of \mathbf{y} has an upper bound:

$$\|\mathbf{y}\|_2 = \sqrt{\sum_{i=1}^d |y_i|^2} = \sqrt{\sum_{i=1}^d (\text{Cov}_{i1}v_1 + \text{Cov}_{i2}v_2 + \cdots + \text{Cov}_{id}v_d)^2} \leq b^2 \cdot c \cdot d \quad (16)$$

In practical applications, different feature columns \mathbf{x}_i may have different bounds b_i . If the cloud service provider has legal access to these bounds, tighter upper bounds can be constructed. In this case, we have $\text{Cov}_{ij} = \frac{1}{n} |\langle \mathbf{x}_i, \mathbf{x}_j \rangle| \leq b_i b_j$, $\|\text{Cov}_i\|_2 \leq \sqrt{\sum_{0 \leq j < d} b_i^2 b_j^2}$, and the upper bound of the Euclidean norm of \mathbf{y} can be expressed as:

$$\|\mathbf{y}\|_2 = \sqrt{\sum_{i=1}^d (\text{Cov}_{i1}v_1 + \text{Cov}_{i2}v_2 + \cdots + \text{Cov}_{id}v_d)^2} \leq \sqrt{\sum_{i=1}^d (\sum_{j=1}^d b_i^2 b_j^2) \cdot c^2} \quad (17)$$

Lazy Normalization Based on the upper bound of the Euclidean norm, we design a Lazy Normalization approach to scale the eigenvectors. Let \mathbf{y} be the eigenvector obtained after the first iteration, and denote the upper bound for its Euclidean norm as B . We then set the interval for the iterative InvSRT algorithm as $(0, B]$. Next, we perform a lower-degree Taylor expansion $T(x)$ of $f(x) = \frac{1}{\sqrt{x}}$ at the midpoint $B + 1$ which serves as the initial approximation function for the iterative InvSRT. It has been proven in [QX] that this Taylor expansion allows the subsequent iterative InvSRT to converge within a finite number of iterations. We use $T(\langle \mathbf{y}, \mathbf{y} \rangle)$ and $\langle \mathbf{y}, \mathbf{y} \rangle$ as inputs for the iteration algorithm and iterate τ times to obtain an approximate accurate value of $\frac{1}{\|\mathbf{y}\|_2}$.

We aim to keep the degree of $T(x)$ as low as possible to minimize the multiplication depth and avoid extremely small high-degree coefficients that may pose representation challenges in homomorphic encryption scenarios. However, due to the significant difference in slopes on both sides of 1 for $\frac{1}{\sqrt{x}}$, the accuracy of $T(x)$ in the interval $(0, 1)$ is lower compared to the interval $[1, B]$. This leads to the fact that values in the $(0, 1)$ interval require more iterations in the subsequent square root reciprocal iteration algorithm to achieve the same level of accuracy as those in the $[1, B]$ interval. Since the $(0, 1)$ interval occupies a very small portion of the entire interval, we choose to base the number of iterations on achieving accurate results in the $[1, B]$ interval and tolerate some error in the $(0, 1)$ interval. Considering that normalization is an amplification process when $\|\mathbf{y}\|_2^2$ belongs to the interval $(0, 1)$, although this amplification cannot be achieved precisely during the iteration process, we can at least require that the output of the iteration algorithm for any input within the interval $(0, 1)$ is greater than or equal to a threshold B' . This helps to control the further substantial reduction of \mathbf{y} .

For any odd-degree Taylor expansion $T(x)$ and any input x in the interval $(0, b^4 \cdot c^2 \cdot d^2]$, it holds that $T(x) \leq \frac{1}{\sqrt{x}}$ [QX]. Furthermore, the output of the iteration algorithm is always smaller than or equal to the true value (Theorem 5). Hence, after Lazy Normalization, we can estimate that both the Euclidean and infinity norms of \mathbf{y} have an upper bound of 1. This allows us to recompute the upper bound of the Euclidean norm for the next approximate eigenvector $\mathbf{y}' = \text{Cov} \cdot \mathbf{y}$ based on the previous calculations. Specifically, if the length of \mathbf{v} , denoted as c , is equal to 1, then the upper bound remains unchanged.

In the final iteration of PowerMethod, in order to generate a more precise normalized eigenvector, we can increase the number of iterations for the Lazy Normalization process or utilize the more accurate function mentioned earlier to obtain an initial estimation. The approach of incorporating additional iterations can also be interleaved within the intermediate iterations of the Power Method, trading more iterations for reduced error. Considering a worst-case scenario where the transformation of Cov consistently diminishes the length of the vector, resulting in underflow of the computed eigenvector, users can request the cloud service provider to scale Cov and alter this situation. Essentially, this adjustment only involves a re-computation of PowerMethod using the scaled version of Cov without the need to start over from the beginning.

Theorem 5. *If Algorithm 4 is given an input $y_0 \leq \frac{1}{\sqrt{x_0}}$, then in any iteration, if $y_{i-1} \leq \frac{1}{\sqrt{x_0}}$ and $y_{i-1} > 0$, it follows that $y_{i-1} \leq y_i \leq x_0$.*

Proof. When $y_{i-1} \leq \frac{1}{\sqrt{x_0}}$ and $y_{i-1} > 0$, we have $0 < x_0 y_{i-1}^2 \leq 1$. Therefore, $y_i \geq y_{i-1}$. On the other

hand, set $y_{i-1} = x_0 - \epsilon$ where $0 \leq \epsilon < \frac{1}{\sqrt{x_0}}$. We can express y_i as follows:

$$\begin{aligned}
y_i &= \frac{1}{2} \left(\frac{1}{\sqrt{x_0}} - \epsilon \right) \left(3 - x_0 \cdot \left(\frac{1}{\sqrt{x_0}} - \epsilon \right)^2 \right) \\
&= \frac{1}{2} \left(\frac{1}{\sqrt{x_0}} - \epsilon \right) (2 + 2\sqrt{x_0}\epsilon - x_0\epsilon^2) \\
&= \frac{1}{\sqrt{x_0}} - \frac{\sqrt{x_0}\epsilon^2}{2} - \sqrt{x_0}\epsilon^2 + \frac{x_0\epsilon^3}{2} \\
&\leq \frac{1}{\sqrt{x_0}}
\end{aligned} \tag{18}$$

□

Algorithm 10 TaylorInit

Input: $ct(\mathbf{x})$ - Encrypted input vector, B - Upper bound for inverse calculation interval, order - Truncation order

Output: $ct(\mathbf{x}')$ - $x'_i = T(x_i) | 0 \leq i < \text{Slots}$, where $T(x)$ is the Taylor expansion polynomial of degree order - 1 of $\frac{1}{\sqrt{x}}$ at $B/2 + 1$.

Algorithm 11 IterativInvSRTbyNewton

Input: $ct(\mathbf{x})$, ciphertext of value x , $ct(\text{Guess})$ initial approximation of InvSRT at point x , τ number of iterations.

Output: $ct(\mathbf{x}')$, $x'_i \approx \frac{1}{\sqrt{x_i}}$

- 1: $ct(\mathbf{x}') \leftarrow ct(\text{Guess})$
 - 2: **for** i range 0 to $\tau - 1$ **do**
 - 3: $ct(\text{Temp}) \leftarrow \text{Mult}(\text{Mult}(ct(\mathbf{x}'), ct(\mathbf{x}')), \text{Mult}(ct(\mathbf{x}'), ct(\mathbf{x})))$
 - 4: $ct(\text{Temp}) \leftarrow \text{Sub}(ct(\text{Temp}), \text{Mult}(pt(3), ct(\mathbf{x}')))$
 - 5: $ct(\text{Temp}) \leftarrow \text{Mult}(pt(1/2), ct(\text{Temp}))$
 - 6: $ct(\mathbf{x}') \leftarrow ct(\text{Temp})$
 - 7: **end for**
 - 8: **return** $ct(\mathbf{x}')$
-

6.1.3 Eigenvalue Computation

The process of computing the eigenvalue is similar to completing another round of Power Method iterations. Let \mathbf{v} be the eigenvector obtained after t iterations. The eigenvalue λ is given by $\lambda = \frac{\langle \text{Cov} \cdot \mathbf{v}, \mathbf{v} \rangle}{\langle \mathbf{v}, \mathbf{v} \rangle}$. We know that \mathbf{v} has been normalized after t iterations. Therefore, if we are confident enough in the accuracy of the normalization process, the eigenvalue computation can be simplified to $\lambda = \langle \text{Cov} \cdot \mathbf{v}, \mathbf{v} \rangle$. The process of $\text{Cov} \cdot \mathbf{v}$ is exactly the same as the first half of a new round of Power Method iterations. However, $\text{Cov} \cdot \mathbf{v}$ and \mathbf{v} have different orientations, i.e., if one is a column vector, the other is a row vector, and vice versa. Therefore, when performing the dot product, we need to flip the orientation of \mathbf{v} to match that of $\text{Cov} \cdot \mathbf{v}$. The axis flipping algorithm (AxisFlipping) is provided in Algorithm (12). Next, computing $\langle \text{Cov} \cdot \mathbf{v}, \mathbf{v} \rangle$ only requires k ciphertext multiplications and one aggregation operation. We can incorporate the eigenvalue computation into the PowerMethod iteration, specifically in the last round of the Power Method (total $t + 1$ rounds), where the iteration is used to compute the eigenvalue instead of updating the eigenvector. Note that we need to retain \mathbf{v}^T to compute the covariance matrix after the eigenvalue transformation.

Algorithm 12 AxisFlipping

Input: A set of square matrices $ct(V[i])|0 \leq i < k$ representing individual vectors, and the axis axis of the vector.

Output: $\{ct(V[i]^T)|0 \leq i < k\}$

```
1: Mask  $\leftarrow I$ 
2: for i range 0 to  $k - 1$  do
3:    $ct(V[i]^T) \leftarrow \text{Mult}(\text{Mask}, ct(V[i]))$ 
4:    $ct(V[i]^T) \leftarrow \text{Aggregate}(ct(V[i]^T); \text{axis} + 1 \bmod 2)$ 
5: end for
6: return  $\{ct(V[i]^T)|0 \leq i < k\}$ 
```

So far, we have discussed the three modules of the Power Method algorithm, namely the linear transformation of the covariance matrix, normalization of the eigenvectors, and computation of the eigenvalues. These modules cover all the processing details of the Power Method, and the complete process is provided in Algorithm (13).

6.2 Privacy-Preserving PCA

The final step is to combine the Power Method with the EigenShift algorithm to compute multiple dominant eigenvectors and their corresponding eigenvalues. The implementation of the EigenShift algorithm is presented in Algorithm (14). It utilizes the eigenvalue λ and the eigenvector and its transpose \mathbf{v}, \mathbf{v}^T obtained in the previous Power Method iteration to update the covariance matrix as $\text{Cov}' = \text{Cov} - \lambda \cdot \mathbf{v}^T \mathbf{v}$. The updated covariance matrix replaces the original one and enters the next round of Power Method computation to compute the next largest eigenvector and its corresponding eigenvalue. The entire process of the Principal Component Analysis algorithm is provided in Algorithm (15).

Modulus Level Refresh Strategy The underlying leveled homomorphic encryption used in our algorithm supports operations up to a limited multiplication depth. When the multiplication depth of our algorithm exceeds the supported depth, we need to refresh the ciphertexts that have reached the maximum depth to shallower levels. This modulus level refreshing can be achieved through two approaches:

1. The service provider sends the ciphertexts that have reached the maximum depth to the user. The user decrypts and re-encrypts the ciphertexts, bringing them back to the initial modulus level. This approach increases the communication overhead and requires the user to wait continuously during the service provider's computation, making it an interactive strategy.
2. The non-interactive strategy: service provider performs bootstrapping locally on the ciphertexts. Bootstrapping is a time-consuming operation, and the runtime of the scheme will be mainly determined by the bootstrapping operation.

Regardless of the chosen modulus-level refresh strategy, its efficiency depends on the number of refresh operations. The computation of the covariance matrix requires at least 6 modulus levels, with an upper limit determined by the matrix multiplication optimization we proposed. As long as the number of levels consumed during this process is kept within the maximum supported depth, no refresh is needed. However, both the PowerMethod and EigenShift algorithms involve operations on the covariance matrix. Thus the modulus level of it becomes an upper bound on the modulus levels of these algorithms and should be kept as high as possible.

Regarding the refresh procedure in the PowerMethod and EigenShift algorithms, we provide a flowchart illustrating the timing of the refresh process. Particularly, when refreshing the approximate eigenvector, we can extract the components of the eigenvector from different ciphertexts and encode them into a single ciphertext, which can then be restored to different ciphertexts after bootstrapping. This approach ensures that the number of refresh operations is independent of the size of the dataset.

Algorithm 13 PowerMethod

Input: Covariance matrix $ct(Cov_i[j])|0 \leq i, j < k$, iterations for Power Method l_P , iterations for Newton Method l_N , initially encrypted submatrices of eigenvectors $ct(V_0[i])|0 \leq i < k$, identifier axis indicating the structure of the current eigenvectors, where 0 represents row vectors with all rows being equal and 1 represents column vectors with all columns being equal, Upper bound for Newton Method B , truncation order for Taylor initialization order.

Output: Maximum eigenvector $ct(V)$ and its transpose $ct(V^T)$ of Cov, along with the maximum eigenvalue $ct(\lambda)$.

```
1: for t range 0 to  $l_P$  do
2:   for i range 0 to k-1 do
3:      $ct(\text{Sum}) \leftarrow ct(\mathbf{0})$ 
4:     for j=0;k;j++ do
5:       if axis == 0 then
6:          $ct(\text{Sum}) \leftarrow \text{Add}(\text{Mult}(ct(Cov_j[i]), ct(V_t[i])), ct(\text{Sum}))$ 
7:       else if axis == 1 then
8:          $ct(\text{Sum}) \leftarrow \text{Add}(\text{Mult}(ct(Cov_i[j]), ct(V_t[i])), ct(\text{Sum}))$ 
9:       end if
10:    end for
11:     $ct(V_{t+1}[i]) \leftarrow \text{Aggregate}(ct(\text{Sum}); \text{axis} + 1 \bmod 2)$ 
12:  end for
13:  axis  $\leftarrow \text{axis} + 1 \bmod 2$ 
14:   $ct(\text{Sum}) \leftarrow ct(\mathbf{0})$ 
15:  for i range 0 to k-1 do
16:     $ct(\text{Sum}) \leftarrow \text{Add}(\text{Mult}(ct(V_{t+1}[i]), ct(V_{t+1}[i])), ct(\text{Sum}))$ 
17:  end for
18:   $ct(\text{Sum}) \leftarrow \text{Aggregate}(ct(\text{Sum}); \text{axis} + 1 \bmod 2)$ 
19:  if  $n < l_P$  then
20:     $ct(\text{Guess}) \leftarrow \text{TaylorInit}(ct(\text{Sum}), B, \text{order})$ 
21:     $ct(\text{Sum}) \leftarrow \text{InvSqrtByIteration}(ct(\text{Guess}), ct(\text{Sum}), l_N)$ 
22:    for i range 0 to k-1 do
23:       $ct(V_{t+1}[i]) \leftarrow \text{Mult}(ct(V_{t+1}[i]), ct(\text{Sum}))$ 
24:    end for
25:  end if
26:  if  $t = l_P$  then
27:     $\{ct(V_t[i]^T)|0 \leq i < k\} \leftarrow \text{AxisFlipping}(\{ct(V_t[i])|0 \leq i < k\}, \text{axis} + 1 \bmod 2)$ 
28:     $ct(\text{Sum}) \leftarrow ct(\mathbf{0})$ 
29:    for i range 0 to k-1 do
30:       $ct(\text{Sum}) \leftarrow \text{Add}(\text{Mult}(ct(V_{t+1}[i]), ct(V_t[i])), ct(\text{Sum}))$ 
31:    end for
32:     $ct(\lambda) \leftarrow \text{Aggregate}(ct(\text{Sum}); \text{axis} + 1 \bmod 2)$ 
33:  end if
34: end for
35: return  $ct(\lambda), \{ct(V_{l_P-1}[i]^T)|0 \leq i < k\}, \{ct(V_{l_P-1}[i])|0 \leq i < k\}$ 
```

Theorem 6. The multiplication depth of Algorithm 13 is $O(l_P \cdot (3 + \log(\text{order}) + 3 \cdot l_N + 1) + 2)$, and the time complexity is dominated by the number of ciphertext multiplications $O(k^2 + k + \log(\text{order}) + 4 \cdot l_N)$ and the number of ciphertext rotations $O(2\log(k))$.

Algorithm 14 EigenShift

Input: Dominant eigenvalue $ct(\lambda), \{ct(V[i]) | 0 \leq i < k\}$, Dominant eigenvector $\{ct(V[i]^T) | 0 \leq i < k\}$, Covariance Matrix $\{ct(Cov_i[j]) | 0 \leq i, j < k\}$

Output: $\{ct(SCov_i[j]) | 0 \leq i, j < k\}$ Eigen-Shifted Covariance Matrix

```
1: for  $0 \leq j < k$  do
2:   for  $0 \leq i < k$  do
3:      $ct(\lambda \cdot V^T V_i[j]) \leftarrow \text{Mul}(ct(\lambda), \text{Mul}(ct(V[j]^T), ct(V[i])))$ 
4:      $ct(SCov_i[j]) \leftarrow \text{Sub}(ct(Cov_i[j]), ct(\lambda \cdot V^T V_i[j]))$ 
5:   end for
6: end for
7: return  $\{ct(SCov_i[j]) | 0 \leq i, j < k\}$ 
```

Algorithm 15 Privacy-Preserving PCA

Input: Maximum eigenvalue, maximum eigenvector, and its transpose: $ct(\lambda), ct(V[i]) | 0 \leq i < k$, $ct(V[i]^T) | 0 \leq i < k$, covariance matrix $ct(Cov_i[j]) | 0 \leq i, j < k$.

Output: $ct(SCov_i[j]) | 0 \leq i, j < k$, the covariance matrix after eigenvalue transformation.

```
1: for  $m:=0; m \leq l_E; m++$  do
2:    $\{ct(V_0[i]) | 0 \leq i < k\} \leftarrow$  Randomly Generate with  $\ell_2 = 1$ 
3:    $axis \leftarrow 1$ 
4:    $ct(\lambda_m), \{ct(V)\}_m, \{ct(V^T)\}_m \leftarrow \text{PowerMethod}(\{ct(Cov_j[\ell])\}, l_P, l_N, \{ct(V_0[i])\}, axis, B, \text{order})$ 
5:    $\{ct(Cov)\} \leftarrow \text{EigenShift}(ct(\lambda_m), \{ct(V)\}_m, \{ct(V^T)\}_m, \{ct(Cov)\})$ 
6: end for
7: return  $\{\{ct(V[i]) | 0 \leq i < k\}_j | 0 \leq j < l_E\}, \{ct(\lambda_j) | 0 \leq j < l_E\}$ 
```

7 Implementation

Our experiments were conducted using the full RNS CKKS approximate numerical homomorphic encryption scheme implemented in Lattigo V4.1.0. All experimental data were obtained using a machine equipped with an AMD Ryzen 7 7735HS with Radeon Graphics (3.19 GHz) processor, running on a 64-bit Windows 10 operating system with 32 GB of memory. We conducted our experiments on the MNIST [Den12], Fashion-MNIST [XRV17], and YALE [BHK97] datasets, which were also used in the experiments of [Pan21]. The preprocessing of the three datasets, including cropping, was performed exactly as described in [Pan21]. The images in the MNIST and Fashion-MNIST datasets were cropped to 16x16 pixels, and the Yale samples were converted to grayscale and cropped from 195 x 231 pixels to 16x16 pixels. We divided these datasets into submatrices of size 128 x 128. We scaled all samples in these datasets by a factor of 1/255, resulting in all features having a maximum value of 1. According to the lazy normalization method, we set the evaluation interval of the InvSRT function to $[0.1^{-7}, 2^{16}]$. The number of iterations is set to 12 to 15 rounds in the Lazy Normalisation. For the interval $[0.1^{-7}, 1]$, 12 rounds ensure that the output for any input in the interval is within the range $[1.04, 0.8]$, while 15 rounds ensure an output range of $[3.8, 2.5]$. For the interval $[1, 2^{16}]$, 12 iterations are sufficient to guarantee a multiplication error of $< 0.1^{-2}$ across the entire interval (and $< 0.1^{-4}$ in the subinterval $[12, 2^{16}]$), while 15 iterations guarantee a multiplication error of $< 0.1^{-4}$ across the entire interval.

We compared our approach with [Pan21] in terms of performance on different datasets (and sample sizes). The main variables include sample size, different numbers of principal components, and the number of iterations for the PowerMethod. In the table, l_E represents the desired number of principal components, l_P represents the number of iterations for the PowerMethod, "Depth" represents the maximum modulus level available in the homomorphic scheme, and "Refresh" represents the number of refresh operations required. Our approach's runtime consists of two parts: the computation time of the covariance matrix (left) and the computation of principal components, i.e., the PowerMethod and EigenShift algorithms (right). Note that the table does not include the time spent on modulus-level refreshment, as its performance depends heavily on different implementation methods, whether it is interactive refreshing or bootstrapping. We provide two measures of principal component accuracy. The first measure is $R2(X)$ used in [Pan21], which represents the R2 score between the reconstructed dataset obtained from privacy-preserving PCA and the original dataset. The second measure, $R2(V)$,

represents the R2 score between the obtained principal components and the ground truth principal components. The "error" followed by these two measurements denotes the error between the result from encrypted data and plaintext. For experiments with sample sizes of 200 and 165, we used 2 threads for computing the covariance matrix, while for the experiment with a sample size of 60,000, we used 7 threads. Our PowerMethod process only used a single thread. The number of threads for computing the covariance matrix depends on the size of the dataset and is limited by the available memory. For larger datasets, such as MNIST with 60,000 samples, our approach with 32 GB of memory and 7 threads already achieves optimal performance, and further increasing the number of threads has minimal impact on efficiency. Having more memory would significantly improve the parallel efficiency of additional threads.

In the interactive refreshing modulus level strategy (Re-enc Mode), we selected a set of homomorphic encryption parameters with $\log N = 15$ and $\log QP = 720$ to achieve 13 effective modulus levels. The rotation key space for matrix multiplication was optimized using the diagonal convergence decomposition technique from Section 3.2, reducing the space requirement from 2294 MB to 1615 MB. The memory usage per instance decreased to 127 MB, with both Z and T being decomposed twice, and the maximum non-zero diagonal index was reduced by a factor of 4. This resulted in additional consumption of four modulus levels, but the speed of linear transformations increased by 22% and 25%, respectively.

Our approach took only two minutes to compute the 200x256 sub-datasets of MNIST and Fashion MNIST, which is four times faster than [Pan21]. In [Pan21], the number of iterations for the square root inverse was fixed at 6, while our PowerMethod circuit can consume fewer modulus levels (refresh times \times depth) to perform more iterations of the square root inverse. Therefore, our approach achieves higher accuracy and is closer to the plaintext results. Additionally, our faster PowerMethod allows us to handle cases where underflows may occur with approximate eigenvectors, as mentioned in Section 6. In such cases, our approach can simply amplify the covariance matrix and recompute the PowerMethod to correct the failure, which is not possible in [Pan21]. Thus, our approach exhibits better "robustness."

Our approach managed to compute the 8 principal components for 60,000 samples of MNIST and Fashion MNIST within an hour, with high accuracy compared to the ground truth principal components. To our best knowledge, no other approach in our research scenario has achieved this scale of computation and efficiency. Furthermore, in our approach, the complexity of the PowerMethod is independent of the sample size and solely determined by the size of the covariance matrix and vector normalization operations. Therefore, we can further increase the number of iterations of the PowerMethod to improve accuracy.

In the Non-interactive strategy (bootstrapping (Btp) Mode), more modulus levels are required to perform the bootstrapping circuit. We selected a set of homomorphic encryption parameters with $\log N = 16$ and $\log QP = 1078 + 465$. Here, 1078 represents the total number of moduli used for bootstrapping, and the remaining 465 bits form 9 layers of 45-bit moduli. The rotation key space for matrix multiplication was optimized using the same strategy as mentioned earlier, reducing the space requirement from 10692 MB to 7524 MB. The memory usage per instance is 225 MB.

To further reduce the number of refreshes, we combined every two iterations of the square root inverse algorithm into a single iteration, reducing the depth per iteration from 3 to 2. This trade-off exchanged additional ciphertext multiplications for fewer modulus levels consumed. With these parameter settings, the overall computation time(except bootstrapping) was roughly twice that of the interactive refreshing modulus-level strategy.

Scheme	DataSet, n	logN	l_E	l_P	depth	Refresh	time	$R2(X)$, <i>error</i>	$R2(V)$, <i>error</i>
[Pan21](Re-enc)	MNIST, 200	15	4	4	11	112	12m	0.141, 0.27	—
Ours(Re-enc)	MNIST, 200	15	4	4	13	91	26s+2m10s	0.460, < 1e-2	-0.246, < 1e-5
Ours(Btp)	MNIST, 200	16	4	4	9	92	1m+4m11s	0.460, < 1e-2	-0.246, < 1e-5
Ours(Re-enc)	MNIST, 60000	15	8	14	13	634	50m+14m	0.317, < 1e-2	+0.728, < 1e-5
[Pan21](Ree-nc)	F-MNIST, 200	15	4	44	11	112	12m	0.411, 0.08	—
Ours(Re-enc)	F-MNIST, 200	15	4	4	13	91	26s+2m14s	0.478, < 1e-2	+0.650, < 1e-5
Ours(Btp)	F-MNIST, 200	16	4	4	9	92	1m+4m10s	0.478, < 1e-2	+0.650, < 1e-5
Ours(Re-enc)	F-MNIST, 60000	15	8	14	13	634	50m+14m	0.577, < 1e-2	+0.911, < 1e-5
Ours(Btp)	F-MNIST, 60000	16	8	14	9	644	2h10m+28m	0.577, < 1e-2	+0.911, < 1e-5
[Pan21](Re-enc)	Yale, 200	15	6	4	11	168	19m	0.411, 0.08	—
Ours(Re-enc)	Yale, 165	15	6	14	13	476	26s+11m	0.674, < 1e-2	+0.810, < 1e-4
Ours(Btp)	Yale, 165	16	6	14	9	483	1m+22m	0.674, < 1e-2	+0.810, < 1e-4

Table 4: Run-time Performance Comparison between [Pan21] and Our scheme under different parameter sets. Notice that [Pan21] did not evaluate their result on the $R2(V)$.

8 Conclusion and further discussion

In conclusion, we first optimized the key space for homomorphic matrix multiplication, reducing the total number of non-zero diagonal vectors and improving the efficiency of rotation operations. We designed circuits for computing the covariance matrix using homomorphic matrix multiplication. Furthermore, we proposed a new homomorphic PowerMethod circuit that takes advantage of the symmetry of the covariance matrix, allowing the linear transformations between the eigenvectors and the covariance matrix to alternate along different axes. We also provided an analysis of the normalization process and introduced a lazy normalization method using the InvSRT iteration algorithm, which offers flexibility and adaptability in PCA parameter deployment.

There are several topics for further discussion, including but not limited to:

1. The performance of PowerMethod depends on the characteristics of the dataset itself, especially the distribution of eigenvalues. If the eigenvalues of the covariance matrix are close to each other, the accuracy of PowerMethod may be reduced. It may be worth considering alternative algorithms like RPCA to achieve more accurate results, but these algorithms often involve computationally expensive components such as QR decomposition, which may result in lower efficiency under the bootstrapping strategy compared to the current scheme.
2. The normalization operation in PowerMethod consumes a significant number of modulus levels. Designing techniques that require fewer modulus levels for normalization could lead to improved efficiency under the bootstrapping strategy.
3. A significant portion of the complexity in homomorphic matrix multiplication comes from row and column transformations. Recent work by Jang et al. (2022) introduced optimizations for matrix multiplication that effectively reduce the complexity of these transformations. Their optimizations could be complementary to ours, and combining them may lead to even better performance.

These topics provide directions for further research and optimization of the proposed homomorphic PCA scheme.

References

- [BGV14] Zvika Brakerski, Craig Gentry, and Vinod Vaikuntanathan. (leveled) fully homomorphic encryption without bootstrapping. *ACM Transactions on Computation Theory (TOCT)*, 6(3):1–36, 2014.
- [BHK97] Peter N. Belhumeur, Joao P Hespanha, and David J. Kriegman. Eigenfaces vs. fisherfaces: Recognition using class specific linear projection. *IEEE Transactions on pattern analysis and machine intelligence*, 19(7):711–720, 1997.
- [BMTPH21] Jean-Philippe Bossuat, Christian Mouchet, Juan Troncoso-Pastoriza, and Jean-Pierre Hubaux. Efficient bootstrapping for approximate homomorphic encryption with non-sparse keys. In *Advances in Cryptology–EUROCRYPT 2021: 40th Annual International Conference on the Theory and Applications of Cryptographic Techniques, Zagreb, Croatia, October 17–21, 2021, Proceedings, Part I*, pages 587–617. Springer, 2021.
- [CHK⁺19] Jung Hee Cheon, Kyoohyung Han, Andrey Kim, Miran Kim, and Yongsoo Song. A full rns variant of approximate homomorphic encryption. In *Selected Areas in Cryptography–SAC 2018: 25th International Conference, Calgary, AB, Canada, August 15–17, 2018, Revised Selected Papers 25*, pages 347–368. Springer, 2019.
- [CK18] Jung Hee Cheon and Andrey Kim. Homomorphic encryption for approximate matrix arithmetic. *Cryptology ePrint Archive*, 2018.
- [Den12] Li Deng. The mnist database of handwritten digit images for machine learning research. *IEEE Signal Processing Magazine*, 29(6):141–142, 2012.
- [DMY16] Dung Hoang Duong, Pradeep Kumar Mishra, and Masaya Yasuda. Efficient secure matrix multiplication over lwe-based homomorphic encryption. *Tatra mountains mathematical publications*, 67(1):69–83, 2016.
- [Hot33] Harold Hotelling. Analysis of a complex of statistical variables into principal components. *Journal of educational psychology*, 24(6):417, 1933.
- [HS14] Shai Halevi and Victor Shoup. Algorithms in helib. In *Advances in Cryptology–CRYPTO 2014: 34th Annual Cryptology Conference, Santa Barbara, CA, USA, August 17–21, 2014, Proceedings, Part I 34*, pages 554–571. Springer, 2014.
- [HS18] Shai Halevi and Victor Shoup. Faster homomorphic linear transformations in helib. In *Advances in Cryptology–CRYPTO 2018: 38th Annual International Cryptology Conference, Santa Barbara, CA, USA, August 19–23, 2018, Proceedings, Part I 38*, pages 93–120. Springer, 2018.
- [JKLS18] Xiaoqian Jiang, Miran Kim, Kristin Lauter, and Yongsoo Song. Secure outsourced matrix computation and application to neural networks. In *Proceedings of the 2018 ACM SIGSAC conference on computer and communications security*, pages 1209–1222, 2018.
- [JLK⁺22] Jaehee Jang, Younho Lee, Andrey Kim, Byunggook Na, Donggeon Yhee, Byoungnan Lee, Jung Hee Cheon, and Sungroh Yoon. Privacy-preserving deep sequential model with matrix homomorphic encryption. In *Proceedings of the 2022 ACM on Asia Conference on Computer and Communications Security*, pages 377–391, 2022.
- [lat22] Lattigo v4. Online: <https://github.com/tuneinsight/lattigo>, August 2022. EPFL-LDS, Tune Insight SA.
- [LKS16] Wen-jie Lu, Shohei Kawasaki, and Jun Sakuma. Using fully homomorphic encryption for statistical analysis of categorical, ordinal and numerical data. *Cryptology ePrint Archive*, 2016.

- [MRDY21] Pradeep Kumar Mishra, Deevashwer Rathee, Dung Hoang Duong, and Masaya Yasuda. Fast secure matrix multiplications over ring-based homomorphic encryption. *Information Security Journal: A Global Perspective*, 30(4):219–234, 2021.
- [Pan21] Samanvaya Panda. Principal component analysis using ckks homomorphic scheme. In *Cyber Security Cryptography and Machine Learning: 5th International Symposium, CSCML 2021, Be’er Sheva, Israel, July 8–9, 2021, Proceedings 5*, pages 52–70. Springer, 2021.
- [Pan22] Samanvaya Panda. Polynomial approximation of inverse sqrt function for fhe. In *Cyber Security, Cryptology, and Machine Learning: 6th International Symposium, CSCML 2022, Be’er Sheva, Israel, June 30–July 1, 2022, Proceedings*, pages 366–376. Springer, 2022.
- [Pea01] Karl Pearson. Liii. on lines and planes of closest fit to systems of points in space. *The London, Edinburgh, and Dublin philosophical magazine and journal of science*, 2(11):559–572, 1901.
- [QX] Hongyuan Qu and Guangwu Xu. Improvements of homomorphic evaluation of inverse square root. *Available at SSRN 4258571*.
- [RMY18] Deevashwer Rathee, Pradeep Kumar Mishra, and Masaya Yasuda. Faster pca and linear regression through hypercubes in helib. In *Proceedings of the 2018 Workshop on Privacy in the Electronic Society*, pages 42–53, 2018.
- [WH19] Shufang Wang and Hai Huang. Secure outsourced computation of multiple matrix multiplication based on fully homomorphic encryption. *KSI Transactions on Internet and Information Systems (TIIS)*, 13(11):5616–5630, 2019.
- [XRV17] Han Xiao, Kashif Rasul, and Roland Vollgraf. Fashion-mnist: a novel image dataset for benchmarking machine learning algorithms. *arXiv preprint arXiv:1708.07747*, 2017.

A Detailed information of full-RNS CKKS scheme

B Proof for the correctness of algorithm DCDforT

Theorem 7. *For a matrix T , Algorithm 6 can decompose T into a product of $\lceil \frac{n-1}{n'} \rceil$ matrices. In this product, any non-zero diagonal of any matrix belongs to the set $0, n, \dots, n' \cdot n$, and there is at most one 1 value in each row and each column of the Boolean matrices.*

Proof. Let’s consider the case of $k = 1$ in Algorithm 6. The algorithm first traverses and decomposes non-zero diagonals $i \cdot n, 0 \leq i \leq n'$ to the $i \cdot n$ diagonal of $T^{(1)}$ and the 0 diagonal of $T^{(0)}$. At this point, the positions where the 0 diagonal of $T^{(0)}$ is set to 1 and the positions where the $i \cdot n$ diagonal of $T^{(1)}$ is set to 1 are given by $i + j \cdot n \bmod n^2, 0 \leq j < n$. Therefore, there are no conflicts in the positions where 1s are set in both $T^{(0)}$ and $T^{(1)}$ for different $i \leq n'$.

The algorithm then traverses and decomposes non-zero diagonals $i \cdot n, n' < i < n$ to the $(i - n') \cdot n$ diagonal of $T^{(1)}$ and the $n' \cdot n$ diagonal of $T^{(0)}$. At this point, the positions where the $n' \cdot n$ diagonal of $T^{(0)}$ is set to 1 are given by $n' \cdot n + i + j \cdot n - n' \cdot n \bmod n^2, 0 \leq j < n$, and the newly set 1 positions in the $(i - n') \cdot n$ diagonal of $T^{(1)}$ are given by $i + j \cdot n \bmod n^2, 0 \leq j < n$. Therefore, there are no conflicts in the positions where 1s are set in both $T^{(0)}$ and $T^{(1)}$ for different $0 \leq i < n$.

We can further generalize this: for any $1 \leq k < \lceil \frac{n}{n'} \rceil$, the positions where 1s are set in the non-zero diagonal set $\{i \cdot n | 0 \leq i \leq n'\}$ for $T^{(1)}$ can be represented as $\{i + j \cdot n \bmod n^2 | 0 \leq j < n\}$ and $\{(i + r \cdot n') + j \cdot n \bmod n^2 | 1 \leq r \leq k, 0 \leq j < n\}$, and the positions where 1s are set in the non-zero diagonal set $\{i \cdot n | n' < i < n - kn'\}$ can be represented as $\{(kn' + i) + j \cdot n \bmod n^2 | 0 \leq j < n\}$. Similarly, The positions where 1s are set in 0-th non-zero diagonal of $T^{(0)}$ can be represented as $\{i + j \cdot n \bmod n^2 | 0 \leq i \leq n', 0 \leq j < n\}$ and $n' \cdot n$ -th non-zero diagonal can be represented as $\{(i + rn') + j \cdot n \bmod n^2 | 0 \leq i \leq n', 1 \leq r \leq k, 0 \leq j < n\}$. Thus, for any k , there are no conflicting positions where 1s are set in the corresponding $T^{(1)}$ (or $T^{(0)}$).

□